Published in final edited form as:

Nature. 2015 January 15; 517(7534): 377–380. doi:10.1038/nature13853.

Control of plant stem cell function by conserved interacting transcriptional regulators

Yun Zhou[1], **Xing Liu**[1], **Eric M. Engstrom**[3,†], **Zachary L. Nimchuk**[1,2,¶], **Jose L. Pruneda-Paz**[4], **Paul T. Tarr**[1], **An Yan**[1], **Steve A. Kay**[5], and **Elliot M. Meyerowitz**[1,2,*]

[1]Division of Biology, California Institute of Technology, 1200 East California Boulevard, Pasadena, CA 91125, United States

[2]Howard Hughes Medical Institute, California Institute of Technology, 1200 East California Boulevard, Pasadena, CA 91125, United States

[3]Biology Department, College of William and Mary, Williamsburg, Virginia 23187–8795, United States

[4]Section of Cell and Developmental Biology, Division of Biological Sciences, University of California San Diego, La Jolla, CA 92093, USA

[5]University of Southern California, Molecular and Computational Biology, Department of Biological Sciences, Dana and David Dornsife College of Letters, Arts and Science, Los Angeles, CA 90089, United States

SUMMARY

Plant stem cells in the shoot apical meristem (SAM) and root apical meristem (RAM) provide for postembryonic development of above-ground tissues and roots, respectively, while secondary vascular stem cells sustain vascular development[1–4]. WUSCHEL (WUS), a homeodomain transcription factor expressed in the rib meristem of the SAM, is a key regulatory factor controlling stem cell populations in the *Arabidopsis* SAM[5–6] and is thought to establish the shoot stem cell niche via a feedback circuit with the CLAVATA3 (CLV3) peptide signaling pathway[7]. WUSCHEL-RELATED HOMEOBOX5 (WOX5), specifically expressed in root quiescent center (QC), defines QC identity and functions interchangeably with WUS in control of shoot and root stem cell niches[8]. WOX4, expressed in *Arabidopsis* procambial cells, defines the vascular stem cell niche[9–11]. WUS/WOX family proteins are evolutionarily and functionally conserved throughout the plant kingdom[12] and emerge as key actors in the specification and maintenance of

*Correspondence and requests for materials should be addressed to E.M.M. (meyerow@caltech.edu).

†Current address: Department of Biology, Rollins College, Winter Park, FL 32789

¶Current address: Department of Biological Sciences, Latham Hall RM 408, Virginia Tech, 220 Ag Quad Lane, Blacksburg, VA 24061

Author contributions

Y.Z. and E.M.M. conceived the experiments. Y.Z., X.L., E.M.E., and A.Y. performed experiments. J.L.P.-P. and S.A.K. provided the transcription factor library. Z.L.N. and P.T.T. contributed reagents. Y.Z., X.L. and A.Y. analyzed data. Y.Z. and E.M.M. wrote the manuscript and X.L., Z.L.N., A.Y. revised it. All the authors have read and approved the manuscript.

The authors declare no competing financial interests.

stem cells within all meristems[13]. However, the nature of the genetic regime in stem cell niches that centers on WOX gene function has been elusive, and molecular links underlying conserved WUS/WOX function in stem cell niches remain unknown. Here we demonstrate that the *Arabidopsis HAIRY MERISTEM* (*HAM*)family transcription regulators act as conserved interacting co-factors with WUS/WOX proteins. HAM and WUS share common targets *in vivo* and their physical interaction is important in driving downstream transcriptional programs and in promoting shoot stem cell proliferation. Differences in the overlapping expression patterns of WOX and HAM family members underlie the formation of diverse stem cell niche locations, and the HAM family is essential for all of these stem cell niches. These findings establish a new framework for the control of stem cell production during plant development.

To identify the molecular mechanism underlying WUS functions in stem cells, we screened for WUS-interacting transcription co-factors using yeast-two-hybrid assays with a transcription factor library[14], and found HAIRY MERISTEM1 (HAM1) strongly and specifically interacting with WUS(Fig. 1a). *HAM* genes, encoding GRAS domain transcription regulators, contribute to shoot stem cell function in petunia and *Arabidopsis*[15–17]. Four *HAM* genes (*HAM1-HAM4*) have been identified in *Arabidopsis*[16], and further yeast assays revealed that WUS also interacted with three other HAM family members (Extended Data Fig. 1a). WUS-HAM associations were confirmed by bimolecular fluorescence complementation (BiFC) assays in tobacco (*Nicotiana benthamiana*), where WUS and HAM were fused to the N- and C-terminal halves of green fluorescent protein (GFP), respectively. Strong GFP fluorescence in nuclei was observed when GFPn-WUS was co-transformed with GFPc-HAM (Fig. 1b–c, Extended Data Fig. 1b–e). WOX4 and WOX5 also interacted with HAM protein sin BiFC assays (Fig. 1d, Extended Data Fig. 1f–q). These WOX-HAM interactions were further confirmed through *in vitro* pull-down assays, where glutathione S-transferase (GST)-WOX4 but not GST bound HAM4-His_6, and GST-WUS but not GST bound HAM1-His_6 (Fig. 1e). Interactions *in planta* were then tested using co-immunoprecipitation assays in tobacco, where WUS-GFP bound FLAG-HAM1 (Fig. 1f) and FLAG-HAM2 (Fig. 1g), GFP-WOX4 bound FLAG-HAM4 (Fig. 1h), and WOX5-GFP boundFLAG-HAM2 (Fig. 1i). In short, with multiple approaches, our work revealed physical interactions between HAM and WUS/WOX family members.

We next constructed various deleted derivatives of HAM1 and WUS for yeast-two-hybrid assays to identify essential regions for their interactions. Deleting amino acids from 117 to 230(D117-230) in HAM1abolished the interaction (Extended Data Fig. 2a). This N-terminal fragment is important for HAM1 function in stem cell maintenance, asHAM1 (D117-230)did not complement the *ham1;2;4*early termination phenotype, while full-length HAM1 driven by the same *HAM1* promoter did(Extended Data Fig. 2b–g), and it is conserved in HAM proteins from *Arabidopsis* and across different plant species (Extended Data Fig. 2h–j). Deletion analyses of WUS identified a C-terminal region required for interaction with HAM1 (Extended Data Fig. 3a), which is also required for WUS function (Extended Data Fig. 3b–d) and is conserved in different plant species (Extended Data Fig. 3e).

To dissect roles of the HAM-WUS interaction in controlling shoot stem cell niches, genetic interactions were analyzed between *ham1;2;3* (lacking function of three of four HAM genes) and the weak *wus* allele *wus-7*(missense mutant) which forms a functional shoot apex[18], similar to wild type in terms of vegetative and inflorescence meristems (Fig. 2a, b, e). Different from*wus-7*single mutants (Fig. 2b) or *ham1;2;3* triple mutants (Fig. 2c), *wus-7;ham1;2;3* quadruple mutants display early termination of vegetative meristem development(Fig. 2d), thus resembling *wus* complete loss of function (null) mutants[5]. This effect also occurred in *wus-7/wus-7;ham1/ham1;ham2/ham2;ham3/+* plants, where 41 out of 45 plants showed strong termination of inflorescence and floral meristems, with only leaves (Fig. 2h) or barren pedicels (flowers without carpels) (Fig. 2g) left at the top of the main shoot, a phenotype typical of *wus-1* null mutants[5], but never observed in *wus-7* (Fig. 2e) or *ham1/ham1*, *ham2/ham2*, *ham3/+* (Fig. 2f) plants. Secondary inflorescence meristems initiated from axillary meristems in*wus-7/wus-7;ham1/ham1;ham2/ham2;ham3/+* also terminated prematurely (Extended Data Fig. 4a–b). Additionally, 3 out of 4*wus-7/ wus-7;ham1/ham1;ham2/ham2;ham4/+* plants displayed inflorescence meristem termination and lacked carpels (Extended Data Fig. 4c). A dose-dependent enhancement of stem cell termination was evident in *wus-7;ham1/+;ham2/+;ham3/+*, and *wus-7; ham1/+;ham2/ ham2;ham3/ham3* backgrounds (Extended Data Fig. 4d–f), demonstrating a functional interdependence between WUS and HAM family members in vivo. Down regulation of *HAM1*, *HAM2* and *HAM3* in a *ham4* shoot meristem, through activation of *microRNA171*reported to target *HAM1, HAM2* and *HAM3* genes[19], led to terminated vegetative development (Extended Data Fig. 4g–h)similar to the *wus-1*phenotype, suggesting that WUS alone is not sufficient to maintain SAMs in the absence of *HAM* activity. Lastly, the *wus-1;ham1;2;3* quadruple homozygote resembles a *wus-1*single mutant in several aspects including the vegetative meristem (Extended Data Fig. 4i–l), suggesting that *WUS* and *HAM* genes could act together at the SAM. All these genetic data are consistent with the hypothesis that WUS and HAM function as partners in shoot meristem maintenance.

In addition to genetic interactions, the molecular function of the WUS-HAM interaction was further investigated. First, quantitative RT-PCR results (Fig. 3i) demonstrated that HAM proteins regulate expression of a set of genes including *JAZ5*, *TIP2;2*, *TCP9*, *GRP23* and *TPL*, which were reported to be directly regulated by WUS[20]. These WUS downstream targets were misregulated in *wus-7* or *ham1;2;3* triple mutant in similar manners, and *wus-7* and *ham1;2;3* synergistically regulated their expression (Fig. 2i), consistent with functional physical (Fig. 1) and genetic (Fig. 2a–h) interactions between WUS and HAM. Then, dual luciferase assays were conducted *in planta* to confirm the direct effects of WUS-HAM on target gene expression. Compared to empty vector controls, the target genes examined were moderately (Fig. 2j–k) or barely (Fig. 2l–m) regulated by WUS or HAM alone, but were dramatically affected when WUS and HAM were combined(Fig. 2j–l), indicating a role for WUS-HAM interaction in regulating their transcription activities. Lastly, Chromatin Immunoprecipitation (ChIP) experiments demonstrated *in vivo* association of YFP-HAM2 proteins with *TPL* (Fig. 2n) and *GRP23* promoters (Fig. 2o), genomic regions similar to that reported to associate with WUS protein *in vivo*[20], supporting the notion that HAM family

members are functional WUS cofactors in controlling the shoot stem cell niche via regulation of common target genes.

Consistently with physical and genetic interactions between HAM and WOX members, visualization of *HAM* and *WUS*/*WOX* fluorescent transcriptional reporters revealed that WOX and HAM family expression overlapped *in planta*. In vegetative (Extended Data Fig. 5c–h)and inflorescence meristems (Fig. 3a–c), *HAM1* and *HAM2* expression overlapped with that of *WUS* in the rib meristem. *HAM1*is expressed in rib meristem and peripheral zone but not in the L1 or L2 layers of the central zone (Fig. 3a, Supplementary video. 1), while *HAM2* expression peaks within the center of the rib meristem (Fig. 3b). Similarly to *WUS* (Extended Data Fig. 5a, b), *HAM1* is negatively controlled by the *CLV* signaling, as*HAM1* is expressed throughout *clv3-2* meristems (Fig. 3d). We imaged the *WUS*and*HAM1* or *HAM2* reporters in the same SAMs (Fig. 3e–l). Although expressed broadly, signals from *HAM1* (Fig. 3f) or *HAM2* (Fig. 3j) overlap with *WUS* signals (Fig. 3e, i) in the same rib zone cells (Fig. 3h, l, Extended Data Fig. 5i–p). Since WUS protein was reported to move in the SAM from its site of transcription in the rib domain[21], the WUS and HAM1/HAM2 interaction domain in SAMs could be broader than their transcriptional domain overlap. We also examined the HAM2 translational reporter, *pHAM2::YPET-HAM2*, in the *ham1,2,4* SAM (Fig. 3m–n, Extended Data Fig. 6), which completely complements the *ham1,2,4* triple mutant (Extended Data Fig. 6 a–c), and it showed a pattern similar to the HAM2 transcriptional reporter: strong signal in the center starting from L3 and low or no signal in the L1 (Fig. 3m–n, Extended Data Fig. 6d–e). Taken together, the co-localization of WUS and HAM1/HAM2 in SAMs is consistent with functional WUS-HAM1/HAM2 interactions (Fig. 1, 2).

HAM4 and *WOX4* co-express in the provascular or procambial cell types of various tissues (Fig. 3o–t, Extended Data Fig. 7). In stem transverse sections, *HAM4* expresses specifically in the procambium, overlapping with *WOX4*expression, as well as with the*HAM3* and *HAM1* expression domains (Fig. 3s–t, Extended Data Fig. 7j–l). The tightly co-regulated spatial and temporal*HAM4* and *WOX4* expression patterns are consistent with a WOX4-HAM4 interaction module (Fig. 1h). Both *HAM2* transcriptional and translational reporters (Extended Data Fig. 8) are expressed in root meristem cells including the QC, overlapping with the QC-specific *WOX5* expression domain[8], consistent with the previous reports of cell-type specific transcriptome analyses[22,23], and indicating the possibility of WOX5-HAM2 interactions in roots. Our finding that both WUS and WOX5 interact with HAM2 may be partially accounted for the fact that WUS and WOX5 are interchangeable in controlling SAMs and RAMs[8]. Taken together, distinct and overlapping expression patterns of *HAM* and *WOX* members indicate that specific HAM-WOX pairs function within different stem cell niches throughout the plant.

To address the importance of the entire HAM family in the control of stem cell niches, we generated a *ham1;2;3;4* quadruply homozygous mutant. Compared to wild type, *ham1;2;3;4* plants displayed growth arrest at the early seedling stage, containing short roots and terminated shoots with two small leaf-like structures 26 days after germination (DAG)(Fig. 4a–c, Extended Data Fig. 9a–d); the shoot apices exhibited valley-like shapes at 26 DAG, lacking functional meristems(Fig. 4d); the hypocotyl transverse sections showed clear

vascular defects, and the vascular bundles had reduced numbers of xylem vessels, fibers(dark blue-stained) and phloem cells (red-stained), consistent with a reduction in the stem cell activity necessary for generating these cell types (Fig. 4e–f). Moreover, midveins in *ham1;2;3;4* leaf-like tissues did not differentiate but instead accumulated a dark-staining cell mass (arrow indicated), resembling ground tissue cells (Extended Data Fig. 9e–f). This is similar to but much stronger than the reported *WOX4 RNAi* phenotype[10]. Root meristematic activity is also severely compromised in *ham* multiple mutants. The QC and columella stem cells (CSC) in *ham1;2;3;4* mutants displayed enlarged and irregular shapes (Extended Data Fig. 9g–h), and with incomplete penetrance, the CSCs in *ham1;2;3* mutant differentiate(Extended Data Fig. 9i–l), resembling reported defects in *wox5* mutants[8]. However, the root phenotype of *ham1;2;3* or *ham1;2;3;4* is much more severe than that of *wox5* mutant, suggesting that HAM regulates root meristem development through not only direct interaction with WOX5 but also WOX5-independent pathways. In summary, in diverse meristems, *ham1;2;3;4* mutants display defects that share similarities with mutants lacking WOX activities, supporting the idea that HAM proteins are co-factors for WUS/WOX family-mediated stem cell niche maintenance. Given the evolutionary conservation of plant meristem cell niches and the *WOX*/*HAM* gene families[12, 16], and the fact that WOX-HAM interactions exist in higher plants besides *Arabidopsis*(Extended Data Fig. 10), this work establishes new basis for studying stem cell niches in *Arabidopsis*, and provides a paradigm for meristem cell control regimes likely to be universal in higher plants.

Methods

Plant materials and growth conditions

Arabidopsis thaliana plants were grown in a sunshine soil/vermiculite/perlite mixture under continuous light at 20°C. The mutant lines *ham1;2;3*(triply homozygous for mutant alleles of *ham1-1*, *ham2-1*, and *ham3-1*), *ham1;2;4*(triply homozygous for mutant alleles of *ham1-1*, *ham2-1*, and *ham4-1*), *wus-7*, *wus-1*, *clv3-2* were previously described[5, 16, 18, 24]. *wus-7;ham1;2;3*, *wus-7;ham1;2;4*, *wus-1;ham1;2;3*, and *ham1;2;3;4* mutants were generated through genetic crosses, and identified based on PCR genotyping in the F2 segregating population. Different mutant combinations in an *er* background were chosen for genetic and morphological analyses. All of the phenotypes were confirmed from multiple independent segregation lines to control for differences in ecotype background. The PCR genotyping was performed as previously described[16, 18]. Reporter lines for *pWUS::DsRed-N7* and *pWOX4::YFP* were previously reported[11, 25].

Yeast two-hybrid assay

Yeast transformation and beta-galactosidase assays were performed following the manufacturer's instructions (Clontech). Full-length cDNAs for *WUS*, *HAM1*, *HAM2*, *HAM3*, and *HAM4* were cloned into pENTR/D/TOPOor pCR8 (Invitrogen), and then *WUS* cDNA was Gateway cloned to pDEST32, and *HAM1*, *HAM2*, *HAM3*, and *HAM4* cDNAs were Gateway cloned into pDEST22 using standard LR reactions (Invitrogen). All of the deletion derivatives for WUS or HAM1 were generated through overlapping PCR with the primers listed in methods, cloned into pENTR/D-TOPO or pCR8, and cloned into pDEST32 or pDEST22 through LR recombination (Invitrogen). All clones were sequenced to confirm

they were in-frame and the corresponding deletions before being transformed into yeast. The bait and prey vectors were transformed into yeast strain *MaV203*, and three single transformed colonies per genotype were used as triplicate for the LacZ liquid assay in 96 Deep well plates (Thermo) and OD reading was recorded in 96-well plate reader (Tecan). The LacZ activity was calculated as (OD420×1000)/(OD600 × cell volume in μl × assay time in minutes) following the yeast two hybrid handbook (Clontech), including a standard error from three biological replicates.

BiFC

For BiFC experiments, full-length *Arabidopsis WUS*, *WOX4*, *WOX5*, *HAM1*, *HAM2*, *HAM3*, *HAM4*, *BARD1* and *FAMA* cDNA Gateway clones were recombined into vectors containing each half of GFP (N or C terminus) to generate the fusion proteins (GFPn-WUS, GFPn-WOX4, GFPn-WOX5, GFPn-BARD1, GFPn-FAMA, GFPc-HAM1, GFPc-HAM2, GFPc-HAM3, GFPc-HAM4, GFPc-BARD1, GFPc-FAMA) as previously described[26]. Plasmid pairs for testing the specific interactions (such as GFPn-WUS and GFPc-HAM1) were co-transformed together with the P19 silencing suppressor[27] into *Nicotiana benthamiana* leaves through *Agrobacterium* infiltration. The infiltrated tobacco leaves were stained with propidium iodide (PI) and imaged using a Zeiss LSM 510 Meta confocal microscope two days after infiltration. Green GFP signals in nuclei (which demonstrate the physical interaction) and red PI staining signals (which indicate tobacco cell structure) were captured at the same time from different detection channels. A 488nm laser line was used to stimulate GFP and PI. A 505–530 band pass filter was used to collect GFP signal and a 585–615 band pass filter was used to collect PI signal. BARD1, a nuclear-localized protein, was included as a negative control. FAMA, a bHLH transcription factor, which has been demonstrated to interact with bHLH transcription factors[28], was used as an additional negative control. The positive signals for each pair were confirmed with four independent biological replicates, and representative image sareshown in the figures. The same method was also used for tomato (*Solanum lycopersicum*) proteins, including GFPn-tomato WUS, GFPn- tomato WOX4, and GFPc-tomato HAM.

Co-immunoprecipitation and Western Blot analysis

WUS or *WOX5*cDNA in pCR8 was recombined to pMDC83[29] to generate a WUS-GFP or WOX5-GFP fusion clone. FLAG-HAM1, FLAG-HAM2 and FLAG-HAM4 were PCR amplified with primers 5′-CACCATGgactacaaggacgacgatgacaagggcggtggaagtCCCTTATCCTTTGAAAGGTTTCAAGG -3′, 5′-CTAACATTTCCAAGCAGAGACAGTAACAAGTTC-3′, and with primers 5′-CACCATGgactacaaggacgacgatgacaagggcggtggaagtCCCCTGCCCTTTGAGCAATTT-3′, 5′-TTAACATTTCCAAGCTGAGACAGTA-3′, and with primers 5′-CACCATGgactacaaggacgacgatgacaagggcggtggaagtAAAATCCCTGCATCATCTCCTC -3′, 5′-CTAAAACCGCCAAGCTGATGTGGCAACAAG-3′, respectively. GFP DNA was amplified and sub-cloned in front of WOX4 cDNA in frame to generate a GFP-WOX4 fragment. FLAG-HAM1, FLAG-HAM2, FLAG-HAM4, and GFP-WOX4 were then recombined into pMDC32[29], respectively. For co-immunoprecipitation of WUS-GFP with FLAG-HAM1, WUS-GFP with FLAG-HAM2, GFP-WOX4 with FLAG-HAM4, or WOX5-GFP with FLAG-HAM2 in *Nicotiana benthamiana*, the constructs were introduced into

Nicotiana benthamiana leaves through *Agrobacterium* infiltration. The leaves were harvested two days after infiltration and frozen in liquid nitrogen. For the immunoprecipitation of YFP-HAM2 in *Arabidopsis*, the shoot apices from the transgenic plants *pHAM2::YFP-HAM2* in *ham1,2,4* were harvested. The nuclei from *Arabidopsis* or tobacco were isolated, and then lysed with RIPA buffer (50 mM Tris-HCl, pH 7.5, 150 mM NaCl, 1% NP-40, 0.5% sodium deoxycholate, 0.1% SDS, 3 mM DTT, 2 mM NaF and 1 mM $NaVO_3$, or 50 mM Tris-HCl, pH 8.0, 150 mM NaCl, 1% NP-40, 0.5% sodium deoxycholate, 0.1% SDS for Co-IP GFP-WOX4 with FLAG-HAM4) containing protease inhibitors cocktail (Roche) and 200 μM PMSF by incubation on ice for 30 min followed by brief sonication. Clear lysates were mixed with diluting buffer containing PMSF and protease inhibitors cocktail (50 mM Tris-HCl, pH 7.5, 150 mM NaCl, 3 mM DTT, 2 mM NaFand 1 mM $NaVO_3$, or 50 mM Tris-HCl, pH 8.0, 60 mM NaCl for Co-IP GFP-WOX4 with FLAG-HAM4) (1:5, v:v), immunoprecipitated with GFP-Trap® agarosebeads (ChromoTek), and the beads were washed three times with the diluting buffer in spin columns (BioRad). The recovered proteins were eluted from the beads by boiling in 2× SDS sample buffer, separated by SDS-PAGE and transferred to nitrocellulose membrane (Millipore). Proteins were detected using anti-GFP antibody (Roche, Cat #11814460001), anti-FLAG antibody (Sigma, Cat # F1804), and HRP conjugated anti-mouse antibody (Promega, Cat # W4021). The co-immunoprecipitation experiments were repeated twice with similar results.

Protein expression constructs and protein purification

WOX4 cDNA was amplified with primers 5′-CATAGAATTCATGAAGGTTCATGAGTTTTCGAA -3′ and 5′-AGTTGCGGCCGCTCATCTCCCTTCAGGATGGAGAGGA -3′(restriction enzyme sites are underlined), and cloned in frame in pGEX-4T-1 with Eco RI and Not I sites. WOX5 cDNA was amplified with primers 5′-ATTTCCCGGGTATGTCTTTCTCCGTGAAAGGTCG -3′ and 5′-AGTTGCGGCCGCTTAAAGAAAGCTTAATCGAAGATCT -3′(restriction enzyme sites are underlined), and cloned in frame in pGEX-4T-1 with XmaI and Not I sites. WUS cDNA was amplified with primers 5′-CATAGAATTCATGGAGCCGCCACAGCATCAG -3′ and 5′-AGTTGCGGCCGCCTAGTTCAGACGTAGCTCAAGA -3′(restriction enzyme sites are underlined), and cloned in frame in pGEX-4T-1 with Eco RI and Not I sites. HAM1-His_6 tag was generated from PCR with primers 5′-CATAGAATTCATGCCCTTATCCTTTGAAAGGTTTCAAGG -3′ and 5′-AGTTGCGGCCGCCTA*GTGATGATGATGATGATG*ACATTTCCAAGCAGAGACAGTA ACAAGTTCTT -3′(restriction enzyme sites are underlined, and HIS_6 coding sequence is italic), and cloned in frame with thrombin cutting site in pGEX-4T-1 with Eco RI and Not I. HAM4-His_6 tag was generated from PCR with primers 5′-CATAGAATTCATGAAAATCCCTGCATCATCTCCTC -3′ and 5′-AGTTGCGGCCGCCTA*GTGATGATGATGATGATG*AAACCGCCAAGCTGATGTGGCA ACAAG -3′(restriction enzyme sites are underlined, and HIS_6 coding sequence is italic), and cloned in frame with thrombin cutting site in pGEX-4T-1 with Eco RI and Not I. All proteins were expressed in Rosetta™ E. Coli (Novagen®) by inducing with 0.4 mM IPTG at 16 °C for 2–4 hours. GST-WOX4, GST-WOX5 and GST were purified on glutathione resin. HAM1 was purified on glutathione resin followed by digestion with thrombin and

chromatography on S200 resins as described previously[30–31]. HAM4 was purified on glutathione resin followed by digestion with thrombin and removal of the GST associated with glutathione resin as described previously[31].

In vitro pull-down assay

GST-WOX4, GST-WOX5, GST-WUS or GST were immobilized on glutathione resin and incubated with HAM1-His_6 or HAM4-His_6 for 30 min at 4 °C. The glutathione resin was then washed three times and processed for SDS-PAGE analysis and western blot analysis using antibody to His-tag (Qiagen, Cat. # 34660). The pull-down experiments were repeated twice with similar results.

Transactivation assay in tobacco

A 60 base pair minimal 35S fragment (the −60 minimal promoter) was amplified and cloned with Bam HI /Nco I sites into the pGREEN800II LUC[32] to generate a pGREEN800II-60LUC. *TPL* promoter was PCR amplified from Col-0 genomic DNA with primers 5′-AACAGGTACCGAACGCTTCGTTTCATTAGTTTATC -3′ and 5′-AATAGGATCCGTTTTCTCTCACTTCCTTAAAAGACT -3′ (restriction enzyme sites are underlined)and cloned with Kpn I /Bam HI sites into the pGREEN800II-60LUC. *TIP2;2* promoter was amplified with primers 5′-AACAGGTACCCGAGTGAAGCAGATTGGGAGAGAA -3′ and 5′-AATACTGCAGTTTGATCCGACAAAATAACTCTGTT -3′ and cloned with KpnI /PstI sites into the pGREEN800II-60LUC. *GRP23* promoter was amplified with primers 5′-AACAGGTACCCAGGTGTGATTGTCAATAGACTACG -3′ and 5′-AACAGATATCGGTGGAGGGAAAATGATTTAGGGTT -3′ and cloned with KpnI /Eco RV sites into the pGREEN800II-60LUC. *TCP9* promoter was amplified with primers 5′-AACAGGTACCGTATGCTGATGGTAGGCAAAAGTT-3′ and 5′-AATACTGCAGTAAAATATAGCTGAGAGAAAACG-3′ and cloned with KpnI /PstI sites into the pGREEN800II LUC. The different reporter constructs (dual-luciferase reporter with different gene promoters) and indicated effectors (empty effector vector or WUS or HAM2, or WUS together with HAM2) were introduced into *Nicotiana benthamiana* leaves through *Agrobacterium* infiltration. The activities from firefly luciferase (LUC) and Renilla luciferase (REN) were quantified two days after infiltration with a Dual Luciferase Assay kit (Promega), and luminescence was recorded using a 96-well dual injection luminometer (Tecan). The LUC activity was normalized to the REN activity (LUC/REN). The means and standard errors of LUC/REN were calculated from three independent biological replicates.

Plasmid constructions for the transgenic plants

It has been reported that *HAM1*, *HAM2* and *HAM3* are targeted and repressed by the *microRNA171* family[19]. To generate new microRNA-sensitive fluorescence reporters for *HAM1*, *HAM2* and *HAM3*, an approach similar to that in a previous report[33] was used. Briefly, a 2xYPET-N7mirS fragment was generated through PCR amplification, which contains a 2x version of YPET with a N7 nuclear localization sequence (2xYPET-N7) followed by 26 base pairs of microRNA target sequence

(GCAAGGGATATTGGCGCGGCTCAATC) from the *HAM* family. These 26 base pairs are recognized and targeted by the microRNA171 family[19, 34].

For the construction of the *pHAM1::2xYPET-N7mirS* reporter, a 4 kb AscI fragment containing the *HAM1* promoter was amplified from Col-0 genomic DNA with primers 5′-TACAGGCGCGCCTTTCCCTCACTTTTTCTTACATTGAA-3′ and 5′-TACAGGCGCGCCACGCCTCCTCAACAACACAGAGTAA-3′(restriction enzyme sites are underlined), and cloned 5′ of the 2xYPET-N7mirS fragment. The fused DNA fragment was introduced into the pMOA34 binary vector[35]. For the construction of *pHAM2::2xYPET-N7mirS*, 3122 bp *HAM2* promoter was amplified with 5′-TACAGTTTAAACAGCAGGACATATCTAAACCAGAAGTT-3′ and 5′-TACAGTTTAAACGACCAATCTTACAGAGTCAGAAAGAG-3′ (restriction enzyme sites are underlined) and cloned in front of *2xYPET-N7mirS*; and 1149 bp HAM2 3′-untranslated sequence was PCR amplified with 5′-TACAGGCGCGCCGACGAAAAAGGAGGATATTTTCACGGT-3′ and 5′-TACAGGCGCGCCACTATGTTTCCATGTACTGTGGGATA-3′(restriction enzyme sites are underlined) and cloned 3′ of the *2xYPET-N7mirS* construct, then the fused DNA fragment was cloned into pMOA34. For the construction of *pHAM3::2xYPET-N7mirS*, 3816 bp *HAM3* promoter was amplified with 5′-TACAGTTTAAACTTTATAAGACTTGCTATGGTCGTGAG-3′ and 5′-TACAGTTTAAACTGCAGACGATAAAAAATAGTGTATT-3′ (restriction enzyme sites are underlined) and cloned before *2xYPET-N7mirS*; and 1755 bp *HAM3* 3′-untranslated sequence was PCR amplified with 5′-TACAGGCGCGCCTTTCCACCGGAGTTTCAATTATTAAA -3′ and 5′-TACAGGCGCGCCTTAGTTGAAGGACAAATAACACCAAA -3′ (restriction enzyme sites are underlined) and cloned 3′ of the *2xYPET-N7mirS* fragment, then the fused DNA fragment was introduced into pMOA34. The double reporter lines including *pWUS::DsRed-N7; pHAM1::2xYPET-N7mirS* line and *pWUS::dsRed-N7; pHAM2::2xYPET-N7mirS* line were generated through genetic crosses.

For the construction of *pHAM4::2xYPET-N7* reporter, 6413 bp *HAM4* promoter was amplified with primers 5′-TACAGGCGCGCCAAATATAAAATAGAATCAAACAAAGTTGGTAAC-3′ and 5′-CAAAGGCGCGCCGTGTTGTGTGTTAAGAAGAAAGAAAGGTGGAGCCTTT-3′ (restriction enzyme sites are underlined), and cloned 5′ of a *2xYPET-N7* fragment, then the fused DNA fragment was cloned into pMOA34.

For the complementation of *wus-1*, a full-length *WUS* or *WUS* derivative without base pairs encoding amino acids from 203 to 236 was cloned into pMOA36 binary vector, together with a 4.4 kb of *WUS* upstream regulatory sequence and 1.5 kb *WUS* 3′-untranslated sequence. The construct was introduced into *wus-1/+* plants using the floral dip method. For the complementation of *ham1,2,4*, *HAM1* or *HAM1* derivative without 117–230 was cloned into pMOA34 binary vector, with a 3949 bp of *HAM1* upstream regulatory sequence and 1387 bp *HAM1* 3′-untranslated sequence. The construct was introduced into *ham1,2,4* plants using the floral dip method.

To generate a *microRNA171* expression construct in shoot meristems, the *microRNA171* DNA was amplified with 5′-CACCTGAGCGCACTATCGGACATCAAA-3′ and 5′-TAAACGCGTGATATTGGCAC-3′ and cloned into pMOA36 together with a 4.4 kb of *WUS* upstream regulatory sequence and 1.5 kb *WUS* 3′-untranslated sequence. The construct was introduced into the *ham4* mutant through the floral dip method. Five independent transgenic plants (*pWUS::mirRNA171* in *ham4*) showing terminated vegetative meristems were identified.

Confocal imaging of fluorescence reporters in living plants

All of the fluorescent reporters were imaged by using a Zeiss LSM 510 Meta confocal microscope, except for the fluorescent reporters in inflorescence meristems and HAM2 fluorescent reporters in the roots, which were imaged by using a Zeiss LSM 780 Meta confocal microscope. Zeiss LSM software was used for reconstructing the Z-stacks for a projection view. Laser and filter settings were used as described previously[36–38]. To image *HAM4* and *WOX4* reporters, the cotyledons, first leaf, hypocotyls and roots from 7-d-old seedlings and stems from 1-cm bolting plants were used. To image dsRED, YPET and PI simultaneously in SAMs, the multi tracking mode in the ZEISS LSM 780 was used. dsRed was excited using a 561 nm laser line in conjunction with 571–589 nm collection; the YPET was excited using a 514 nm laser line in conjunction with a 519–549 nm collection; and PI was excited using a 514 nm laser with 631–673 nm collection. There is no spectral bleed-through of DsRed into the YPET collection channel, nor YPET into the DsRed collection channel under these settings, and for better display, all images from dsRed channel are equally enhanced with the same scale and all images from the PI channel are uniformly enhanced to the similar intensity using Image J software.

Histology

The wild type and *ham1;2;3;4* seedlings were fixed in 4% paraformaldehyde, dehydrated and embedded in Paraplast X-tra (Fisher). The samples in wax were sectioned at 8 microns, de-waxed and dehydrated, and the slides were stained with Alcian blue together with Safranin O (red) as previously described[39], to detect non-lignified cell walls and lignified cell walls, respectively.

Real-time RT-PCR analysis

Total RNA was isolated from 10-day old plants with roots, hypocotyls and leaves dissected off, using the RN easy Kit (Qiagen). SuperScript III reverse transcriptase (Invitrogen) was used to synthesize the first-strand cDNA with oligo (dT) primer and 1 μg of total RNA at 50°C for 1 h. Quantitative PCR was then performed with the Sensi Mix SYBR Hi-ROX Kit (Bioline) on Roche Real-Time PCR machine following the manufacturer's instruction. The thermal cycling program was 95°C for 10 min, followed by 45 cycles of 95°C for 10 s, 56°C for 30 s, 72°C for 40s, and a one-cycle dissociation stage at 95°C for 15 s, 60°C for 1 min, and 97°C for 15 s. The primers used in quantitative RT-PCR were *JAZ5*, 5′-GAAAGACAGAGCTGTGGCTAGG -3′ and 5′-TTGGCCTTCTTCAATCTTCATAATA -3′; *TIP2;2*, 5′-ACCAATGGCGAGAGCGTACCG -3′ and 5′-ATGAAACCGATAGCAATTGGAG -3′; *TCP9*, 5′-ACCTCCTTTACAAGTTGTTCCAAG

-3′ and 5′-TGAAGCTCTTGTTTCTCGTATATCTC -3′; *GRP23*, 5′-AGACAGCTAGCCATCAGCAGTCAC -3′ and 5′-AGTTCCTCAACTCCACTACCTTTTT -3′; *TPL*, 5′-AGCTAGTCTCAGCAATTCAAA -3′ and 5′-AGGCTGATCAGATGCAGAGG -3′; and *UBQ10*, 5′-AACAATTGGAGGATGGTCGT -3′ and 5′-TTCCAGGGAAGATGAGACG-3′. Fold change was calculated as $2^{\Delta\Delta Ct}$ and standard error was calculated from three biological replicates, and each biological replicate was examined in triplicate.

Chromatin immunoprecipitation(ChIP)

For the construction of *pHAM2::YFP-HAM2* (*pHAM2::YPET-HAM2*), the YFP variant YPET was amplified and cloned in front of *HAM2* cDNA in frame to generate *YFP-HAM2* fragment. Then the 3122 bp *HAM2* promoter was amplified with 5′-TACAGTTTAAACAGCAGGACATATCTAAACCAGAAGTT-3′ and 5′-TACAGTTTAAACGACCAATCTTACAGAGTCAGAAAGAG-3′ (restriction enzyme sites are underlined) and cloned in front of *YFP-HAM2* and 1149 bp HAM2 3′-untranslated sequence was amplified with 5′-TACAGGCGCGCCGACGAAAAAGGAGGATATTTTCACGGT-3′ and 5′-TACAGGCGCGCCACTATGTTTCCATGTACTGTGGGATA-3′ and cloned 3′ of the *YFP-HAM2*. Then the whole fused DNA fragment (*pHAM2-YFP-HAM2-HAM2 3′UTR*) was cloned into the binary vector pMOA34. The construct was introduced into *ham1,2,4* plants using the floral dip method, and the complemented *ham1,2,4 [pHAM2::YFP-HAM2]* line was selected for the western blot, GFP IP (shown in Extended Data Fig. 6f) and ChIp experiments. ChIP followed by a quantitative real-time PCR approach was used to investigate the *in vivo* association of HAM2 with the *TPL* and *GRP23* promoters as described previously[40] with some modifications. In general, 2 g of *ham1,2,4* (negative control) or *ham1,2,4 [pHAM2::YFP-HAM2]* plants was harvested and fixed with 1% formaldehyde under vacuum. Nuclei were isolated and lysed, and chromatin was sheared to an average size of 500 bp by sonication 7 times for 20 seconds each with a Branson Sonifier. Samples were kept on ice during sonication and were cooled for 1 min between sonication pulses. The sonicated chromatin served as input. Immunoprecipitations (IPs) were performed with GFP-Trap® Agarose beads (Chromotek) at 4°C following the manufacturer's procedure. The precipitated DNA was isolated and purified, and served as a template for PCR. Quantitative PCR was performed as described in real-time RT-PCR analysis. The relative enrichment for each immunoprecipitated amplicon (from *TPL* or *GRP23* promoter) from GFP-TRAP is presented as ChIP/Input ratio, and *TUA4* and *ACT7* (*ACTIN7*) amplicons are also included to serve as negative controls. The ChIp experiments have been conducted three times using independent biological replicates with similar results, and one representative data set with two technical replicates is presented. The primer pairs used in ChIp-PCR are as follows: *TPL Amplicon1*, 5′-GCAATTGGCTCTTCAATGTC -3′ and 5′-GGACGGAGATCTAACGGCTA -3′; *TPL Amplicon2*, 5′-CCATATGACCGGGATATGAGA -3′ and 5′-GGGATATGTCGCTTTCCATT -3′; *TPL Amplicon3*, 5′-TTGAGTCAGGGCTCATCTCC -3′ and 5′-CTTTCGCGAGAACCAACTTC-3′; *GRP23 Amplicon1*, 5′-ACCATCGTCATTGGTTTCGT -3′ and 5′-GGAGGTGACTGAGAGACATGG -3′; *GRP23 Amplicon2*, 5′-CAACAAATTCCTGTTTTCACGTT -3′ and 5′-

CGAAAATGTTCGAACTGCAT -3′; *GRP23 Amplicon3*, 5′-CGCCATCGCCTAAAAGTAAA -3′ and 5′-TTTGTTGGCTAGGCATAGGG -3′; *GRP23 Amplicon4*, 5′-AGACAGCTAGCCATCAGCAGTCAC -3′ and 5′-AGTTCCTCAACTCCACTACCTTTTT -3′; *TUA4 Amplicon*, 5′-CTTTGGTCTTTAGCAGGTTC -3′ and 5′-CCCATCTGTATATAACGACAC -3′; *ACTIN7 Amplicon*, 5′-TGCTTGTTATGTGATTCGATCC -3′ and 5′-GATCGACAGAAGCGAGAAGAAT -3′.

Staining

mPS-PI staining and root imaging of the staining was performed as previously described [41].

SEM

For scanning electron microscopy, tissue was placed in 1.2% glutaraldehyde in 0.025M phosphate buffer (sodium phosphate, pH 6.8), vacuum was applied for 10 min, and tissue was fixed overnight at 4°C. Tissue was then rinsed twice with 0.025M phosphate buffer for 1 h, postfixed with 0.5% osmium tetroxide in 0.025Mphosphate buffer for 24 h at room temperature, and moved through an increasing ethanol series (20% increments), each increment lasting a minimum of 1 h and ending with two exchanges of 100% ethanol. Ethanol was removed by critical point drying with a critical point drier (SAMDRI), and tissue was mounted to stubs with double-sided adhesive tape and sputter coated with gold-palladium alloy using a Hummer Sputtering System (Anatech). Samples were examined with a Hitachi 4700 scanning electron microscope.

Primers used for cDNA clones and deletion constructions

HAM1c/5CACC (5′-CACCATGCCCTTATCCTTTGAAAGGTTTCAAGG-3′); HAM1c/3 (5′-ACATTTCCAAGCAGAGACAGTAACAAG-3′); HAM1c5/231 (5′-CCGTTTTATCACAACAACCAG-3′); HAM1c5/441 (5′-GAAAATCTCAAAACATTCG-3′); HAM1D71-116/5 (5′-AGTCCTCTCGCTTCTTATTCTGCTTCTTCTCCTGGTCAAGAGC-3′); HAM1D71-116/3 (5′-GCTCTTGACCAGGAGAAGAAGCAGAATAAGAAGCGAGAGGACT-3′); HAM1c71/5CACC (5′-CACCATGTCTACCACCACCACGCTGTCTTCCTCT-3′); HAM1D117-230/5 (5′-GATGATCTTGACGGTGTTCTCTCTCCGTTTTATCACAACAACCAGCAA-3′); HAM1D117-230/3 (5′-TTGCTGGTTGTTGTGATAAAACGGAGAGAGAACACCGTCAAGATCATC-3′); HAM4c/5 (5′-ATGAAAATCCCTGCATCATCTCCTC-3′); HAM4c/3 (5′-AAACCGCCAAGCTGATGTGGCAACA-3′); WUSc5/1 (5′-ATGGAGCCGCCACAGCATCAG-3′); WUSc5/30 (5′-TACACGTGTCGCCAGACCAG-3′); WUSc5/100 (5′-AGATTCAACGGAACAAACATGAC-3′); WUSc5/171 (5′-GCAAGCTCAGGTACTGAATGT-3′); WUSc/3stop (5′-CTAGTTCAGACGTAGCTCAAGA-3′); WUSc3/236 (5′-ACCTTCTAGACCAAACAGAGG-3′); WUSc3/292 (5′-

GTTCAGACGTAGCTCAAGAGAAGC-3′); WUSD164-183/5 (5′-TAACAAGCCATATCCCAGCTTCAATGGCTACATGAGTAGCCATG-3′); WUSD164-183/3 (5′-CATGGCTACTCATGTAGCCATTGAAGCTGGGATATGGCTTGTTA-3′); WUSD101-163/5 (5′-GGCTCGTGAGCGTCAGAAGAAGAGAAATAACGGGAATTTAAATCATGCAA-3′); WUSD101-163/3 (5′-TTGCATGATTTAAATTCCCGTTATTTCTCTTCTTCTGACGCTCACGAGCC-3′); WUSD132-163/5 (5′-TATCATCCTCTACTTCACCATCATAATAACGGGAATTTAAATCATGCAA-3′); WUSD132-163/3 (5′-TTGCATGATTTAAATTCCCGTTATTATGATGGTGAAGTAGAGGATGATA-3′); WUSD184-236/5 (5′-AATGTGGTGTTGTTAATGCTTCTCATCAAGAAGAAGAAGAATGTGG-3′); WUSD184-236/3 (5′-CCACATTCTTCTTCTTCTTGATGAGAAGCATTAACAACACCACATT-3′); WUSD164-236/5 (5′-TAACAAGCCATATCCCAGCTTCCATCAAGAAGAAGAAGAATGTG-3′); WUSD164-236/3 (5′-CACATTCTTCTTCTTCTTGATGGAAGCTGGGATATGGCTTGTTA-3′); WUSD184-202/5 (5′-AATGTGGTGTTGTTAATGCTTCTTACAACAACGTAGGTGGAGGAT-3′); WUSD184-202/3 (5′-ATCCTCCACCTACGTTGTTGTAAGAAGCATTAACAACACCACATT-3′); WUSD203-236/5 (5′-TGGAACAAGACTGTTCTATGAATCATCAAGAAGAAGAAGAATGTGG-3′); WUSD203-236/3 (5′-CCACATTCTTCTTCTTCTTGATGATTCATAGAACAGTCTTGTTCCA-3′); WUSD218-236/5 (5′-GGGCAAACATGGATCATCATTACCATCAAGAAGAAGAAGAATGTGG-3′); WUSD218-236/3 (5′-CCACATTCTTCTTCTTCTTGATGGTAATGATGATCCATGTTTGCCC-3′) WUSD203-217/5 (5′-TGGAACAAGACTGTTCTATGAATTCATCTGCACCTTACAACTTCTT-3′); WUSD203-217/3 (5′-AAGAAGTTGTAAGGTGCAGATGAATTCATAGAACAGTCTTGTTCCA-3′); WOX4c/5CACC (5′-CACCATGAAGGTTCATGAGTTTTCGAA-3′); WOX4c/3stop (5′-TCATCTCCCTTCAGGATGGAGAGGA-3′); WOX5c/5CACC (5′-CACCATGTCTTTCTCCGTGAAAGGTC-3′); WOX5c/3 (5′-AAGAAAGCTTAATCGAAGATCT-3′); TomatoHAM/5CACC (5′-CACCATGATTGTAATACCTCAAAGTAATAA-3′); TomatoHAM/3stop (5′-TTAAAAGAAAATCTCTTCTGGCTTCAGA-3′); ToamtoWUS/5CACC (5′-CACCATGGAACATCAACACAACATAGAAGA-3′); TomatoWUS/3stop (5′-TTAGGGGAAAGAGTTGAGAGTAAGT-3′); TomatoWOX4/5CACC (5′-

CACCATGTACATGGGATCATCATCAGGAAG-3′); TomatoWOX4/3stop (5′-TCATCTCATGCCTTCTGGATGCAATG-3′)

Extended Data

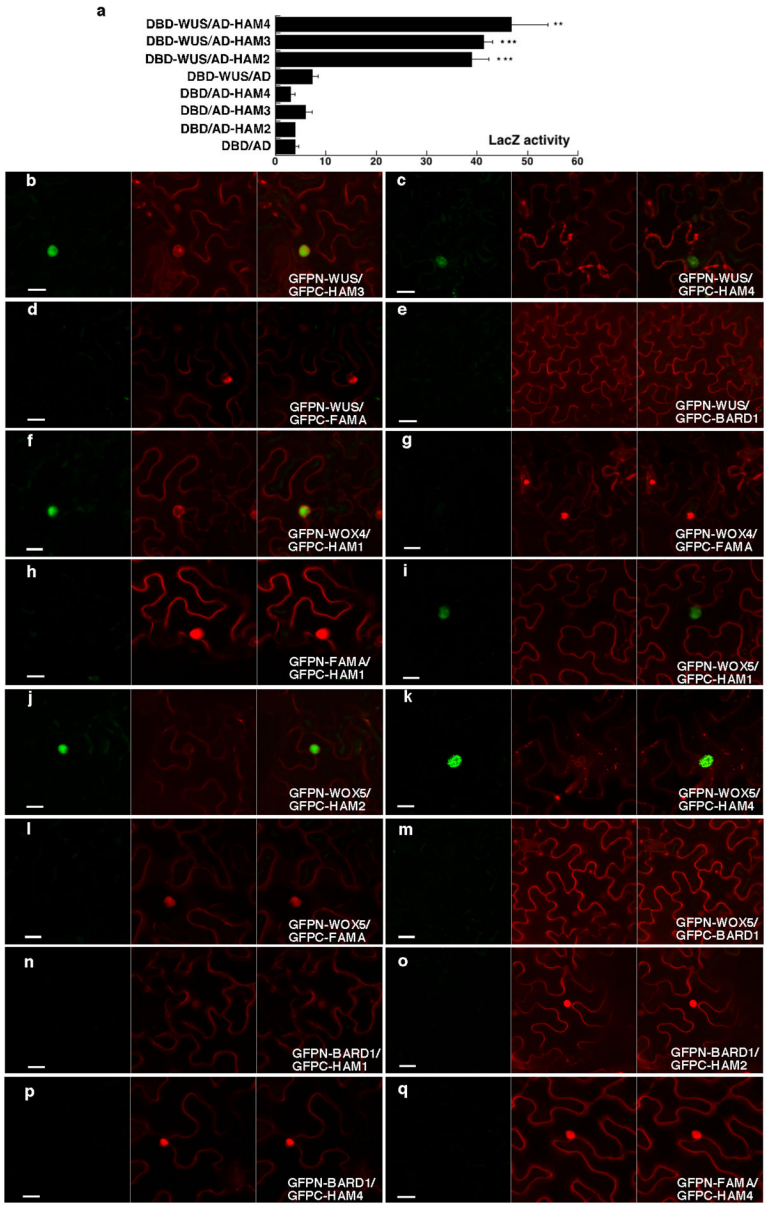

Extended Data Figure 1.

Interaction between WUS/WOX and HAM family transcriptional regulators. (**a**) LacZ activity in yeast-two-hybrid assays testing interactions between WUS and HAM2, HAM3 or HAM4. Error bar = mean ± sem (n=3biological replicates). **, P<0.01; ***, P<0.001(two-tailed t-test, compared to DBD-WUS/AD). (**b**–**o**) Bimolecular fluorescence complementation (BiFC) analyses in tobacco transient assays with HAM and WOX family genes. Tobacco was co-transformed with GFPn-WUS and GFPc-HAM3 (**b**), or GFPn-WUS

and GFPc-HAM4 (**c**), or GFPn-WUS and GFPc-FAMA (**d**), or GFPn-WUS and GFPc-BARD1 (**e**), or GFPn-WOX4 and GFPc-HAM1 (**f**), or GFPn-WOX4 and GFPc-FAMA (**g**), or GFPn-FAMA and GFPc-HAM1 (**h**), or GFPn-WOX5 and GFPc-HAM1 (**i**), or GFPn-WOX5 and GFPc-HAM2 (**j**), or GFPn-WOX5 and GFPc-HAM4 (**k**), or GFPn-WOX5 and GFPc-FAMA (**l**), or GFPn-WOX5 and GFPc-BARD1 (**m**), or GFPn-BARD1 and GFPc-HAM1 (**n**), or GFPn-BARD1 and GFPc-HAM2 (**o**), or GFPn-BARD1 and GFPc-HAM4 (**p**), or GFPn-FAMA and GFPc-HAM4 (**q**). BARD1 and FAMA proteins are both included as negative controls. Left panel: GFP channel; middle panel: propidium iodide (PI) staining channel; right panel: merged channels. Scale bar = 20 μm.

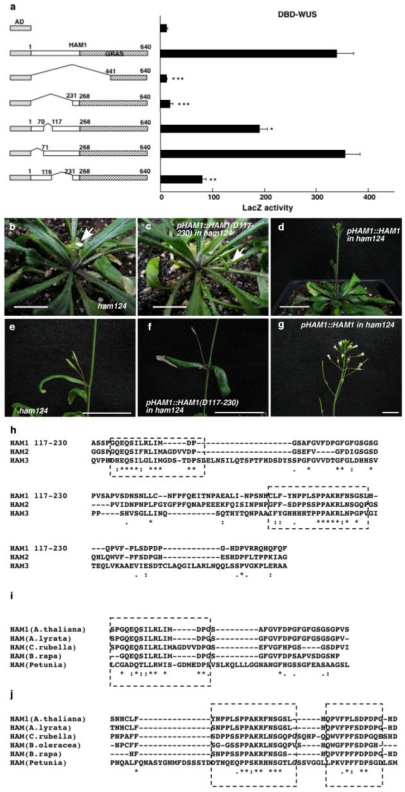

Extended Data Figure 2.

An N-terminal region of HAM1 is important for WUS-HAM1 interactionand is essential for HAM1 function in stem cell maintenance. (**a**) Yeast two-hybrid assay of interactions between WUS and various deleted derivatives of HAM1. Deleting amino acids 117 to 230(D117-230) from HAM1 compromised the WUS-HAM1 interaction. Left panel: box diagrams of the HAM1 derivatives. Shaded boxes indicate the GRAS domains. Numbers indicate amino acid residues. Error bar = mean ± sem (n=3biological replicates). *, P<0.05; **, P<0.01; ***, P<0.001(two-tailed t-test, compared to AD-HAM1 full-length). (**b**–**g**) The complementation of the *ham1;2;4* triple mutant requires amino acids 117-230. The early termination phenotype of *ham1;2;4*(**b, e**) was not complemented by HAM1 (D117-230) driven by a *HAM1* promoter and 3′UTR (**c, f**), but was fully complemented by wild type *HAM1*(**d, g**). Arrows in (**b, c**) indicate the early-terminated inflorescences. (**h**–**j**) Amino acid sequence alignment of the HAM1 N-terminal domains (117–230) using Clustal Omega. (**h**)

Sequence alignment of the N-terminal domains among three *Arabidopsis* HAM members. (**i**) Sequence alignment of partial N-terminal domains in HAM from *A.thaliana*, *A.lyrata*, *C.rubella*, *B.rapa*, and *Petunia*. (**j**) Sequence alignment of partial HAM1 N-terminal domains in HAM from *A.thaliana*, *A.lyrata*, *C.rubella*, *B.oleracea*, *B.rapa*, and *Petunia*. Asterisks: same amino acids; dots: similar amino acids. The conserved regions are boxed. Bars = 10 mm in (**b, c**), and (**g**), 40 mm in (**d**), 20 mm in (**e, f**).

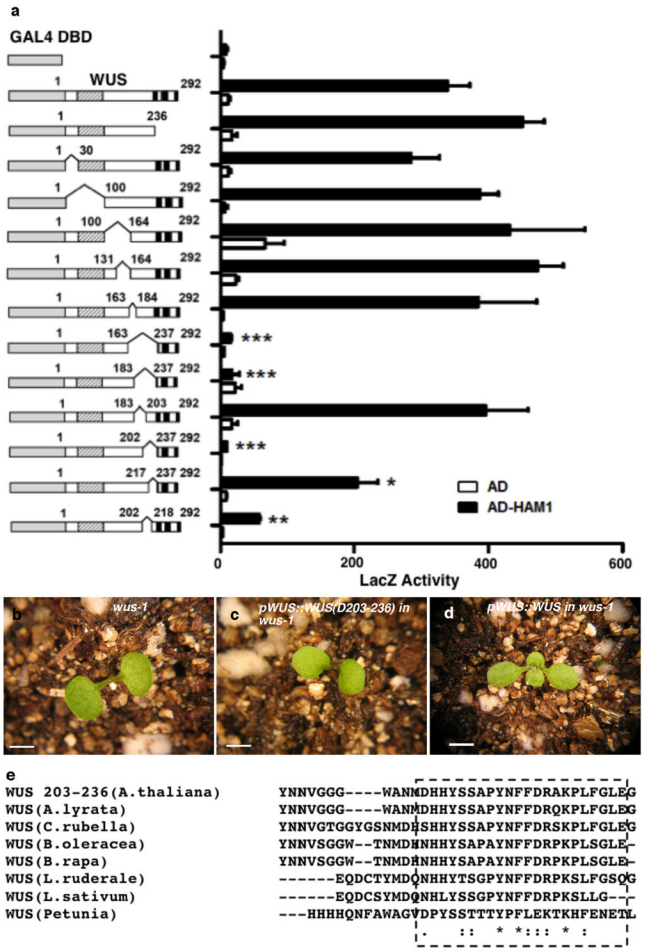

Extended Data Figure 3.

A C-terminal region of WUS is important for WUS-HAM1 interaction and is essential for WUS function in stem cell maintenance. (**a**) Yeast-two-hybrid assay of interactions between HAM1 and various deleted WUS derivatives. Deleting amino acids 203 to 236 (D203-236) from WUS greatly compromised the WUS-HAM1 interaction. Left panel: box diagrams of the deleted WUS derivatives; shaded boxes: the homeodomain; three black boxes: the acidic domains, the WUS box and the EAR motif, respectively. Numbers indicate amino acid residues. Error bar = mean ± sem (n=3biological replicates).*, P<0.05; **, P<0.01; ***, P<0.001(two-tailed t-test, compared to DBD-WUS full-length). (**b**–**d**) WUS function requires the same region that is important for WUS-HAM1 interaction. The terminated shoot meristem phenotype of *wus-1* (**b**) was not complemented by WUS (D203-236) driven by *WUS* promoter and 3′UTR (**c**), and was fully complemented by the wild type *WUS* (**d**). (**e**)

Amino acid sequence alignment of C-terminal regionsof WUS from *Arabidopsis thaliana*, *A.lyrata*, *Capsella rubella*, *Brassica oleracea*, *B.rapa*, *Lepidium ruderale*, *L.sativum*, and *Petunia*, using Clustal Omega. Asterisks: same amino acids; dots: similar amino acids. The conserved regions are boxed. Bars = 2 mm in (**b**–**d**).

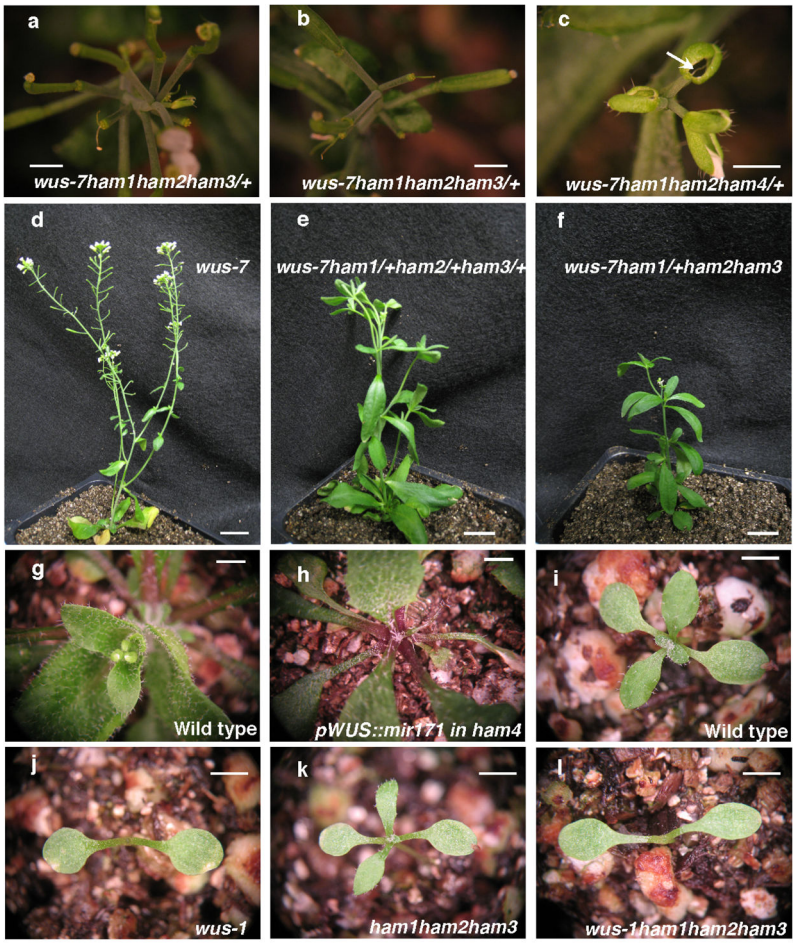

Extended Data Figure 4.

Genetic interaction between WUS and HAM family members. (**a**, **b**) The secondary inflorescence meristems initiated from axillary meristems in *wus-7; ham1;2* homozygotes with *ham3/+* terminate prematurely. (**c**)*wus-7; ham1;2* homozygotes with *ham4/+* display early termination of the main inflorescence meristem and lack of carpels in flowers (indicated by arrow). (**d**–**f**) *WUS* and *HAM* family members interact genetically in a dose-dependent manner. *wus-7* (**d**) formed functional shoot apices and normal stature, but *wus-7; ham1/+; ham2/+; ham3/+* (**e**) enhanced the *wus-7* phenotype, and *wus-7; ham1/+; ham2; ham3* (**f**) showed stronger enhancement, with reduced flower numbers and plant stature, and elongated vegetative stage, resembling a *wus* strong allele. Plants are 36 days after germination. (**g**–**h**) Down-regulation of *HAM1*, *HAM2* and *HAM3* in *ham4* shoot meristems leads to an early termination phenotype. Compared to wild type (Col) (**g**), *pWUS::mir171* in *ham4* (**h**) showed terminated vegetative meristems. (**i**–**l**) WUS is required for functions of HAM1, HAM2 and HAM3. At 11 days after germination, compared to L*er* wild type (**i**) and

ham1;2;3 (**k**) which formed functional vegetative meristem and leaf primordia, *wus-1; ham1;2;3* (**l**) displays terminated vegetative meristems similar to *wus-1* (**j**). Bars = 2 mm.

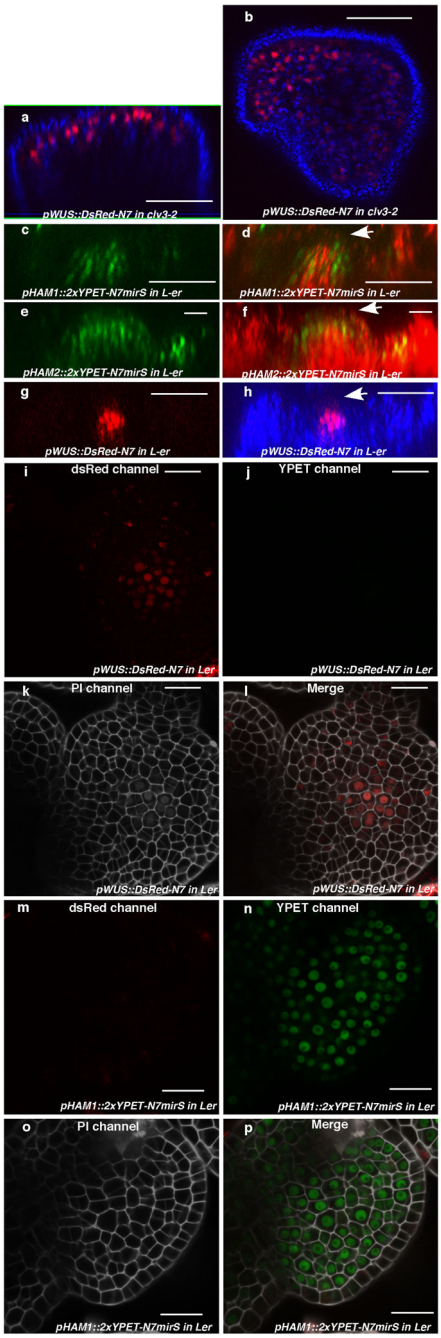

Extended Data Figure 5.

Expression of *HAM1*, *HAM2* and *WUS* in the SAMs. (**a**–**b**) *WUS* expression in *clv3-2*. Orthogonal (**a**) andtop (**b**) views of *pWUS::DsRed-N7* expression (red)and chlorophyll autofluorescence (blue) in the same *clv3-2* inflorescence meristem. (**c**–**h**) Comparison between expression patterns of *HAM1*, *HAM2* and *WUS* in vegetative meristems.(**c**)

Orthogonal view of *pHAM1::2xYPET-N7mirS* expression (green) in L*er* vegetative meristem. (**d**) Orthogonal view of *pHAM1::2xYPET-N7mirS* expression (green) together with chlorophyll autofluorescence (red) in the same vegetative meristem shown in (**c**), indicating that *HAM1* is expressed in the rib meristem. (**e**) Orthogonal view of *pHAM2::2xYPET-N7mirS* expression (green) in L*er* vegetative meristem. (**f**) Orthogonal view of *pHAM2::2xYPET-N7mirS* expression (green) together with chlorophyll autofluorescence (red) in the same vegetative meristem shown in (**e**), indicating that *HAM2* is highly expressed in the rib meristem. (**g**) Orthogonal view of *pWUS::DsRed-N7* expression (red) in L*er* vegetative meristem. (**h**) Orthogonal view of *pWUS::DsRed-N7* expression (red) together with chlorophyll autofluorescence (blue) in the same vegetative meristem shown in (**g**), indicating that *WUS* is expressed in the rib meristem. Arrows indicate the positions of L1 cell layer. (**i**–**p**) Control images confirming the specificity of confocal spectral settings for Fig. 3(**e**–**l**). The SAMs from *pWUS::DsRed-N7* line (**i**–**l**) or *pHAM1::2xYPET-N7mirS* line (**m**–**p**) were imaged from the same three separated channels used in Fig. 3 (**e**–**l**). There is no spectral bleed-through of YPET signal into the ds Red channel (**m**), nor ds Red signal into the YPET channel (**j**). (**i, m**)ds Red channel (red); (**j, n**) YPET channel (green); (**k, o**) PI staining channel (gray); (**l, p**) merged all three channels. Bars = 50μm in (**a**–**d**, **g**–**h**), 20 μm in (**e**–**f**, **i**–**p**).

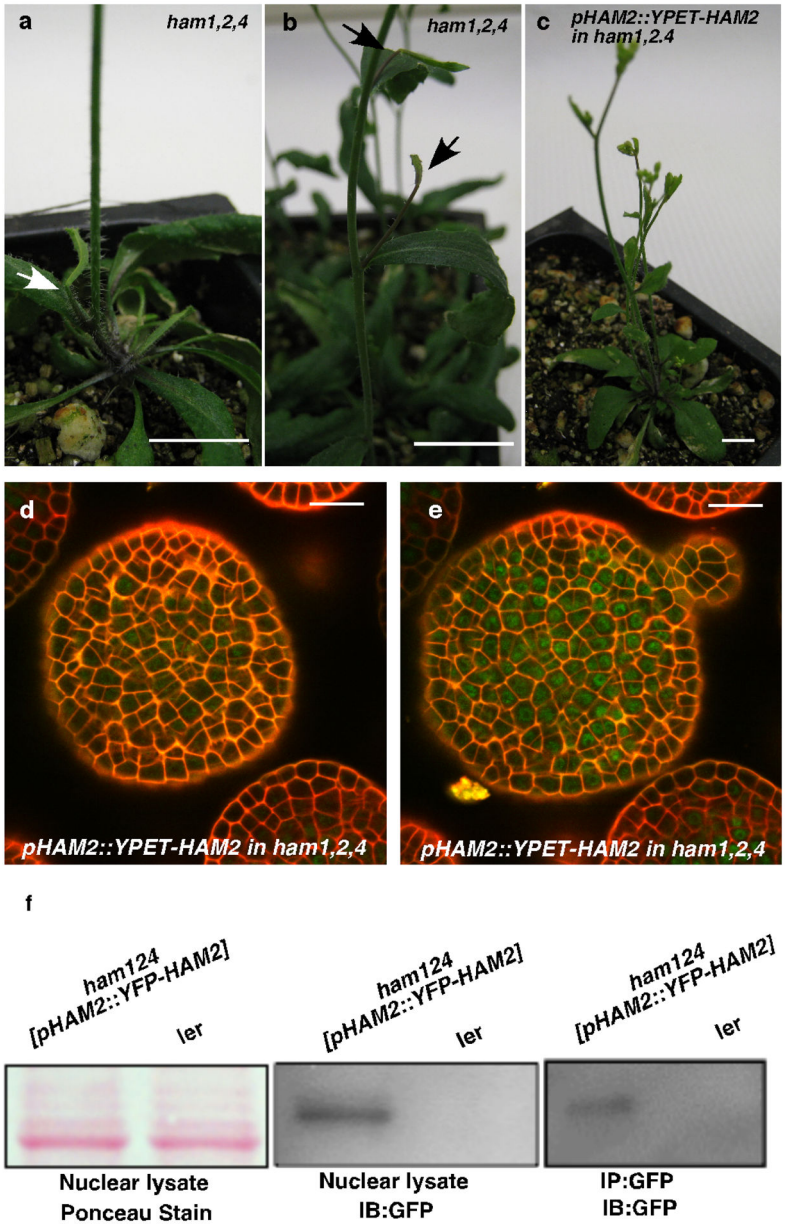

Extended Data Figure 6.

pHAM2::YFP-HAM2 (*pHAM2::YPET-HAM2*)complemented the *ham1,2,4* mutant and was expressed in the center of SAMs. The early termination phenotype of*ham1;2;4*(**a, b**) was completely complemented by YPET-HAM2 driven by the *HAM2* promoter and 3′UTR (**c**), indicating the promoter used for HAM2 transcriptional and translational reporters are functional and the fusion protein (YPET-HAM2) is also functional *in vivo*. Arrows in (**a, b**) indicate early-terminated apices. Bars = 10 mm (**a**–**c**). (**d**–**e**) Different Z sections from the same SAM in *ham1,2,4 [pHAM2::YPET-HAM2]* plant for Fig. 3 (**m**–**n**) show expression of *pHAM2::YPET-HAM2* translationalmarker (green) in L2 (**d**) and L3 (**e**), together with PI as counter stain (Red). Bars = 20 μm (**d**–**e**). (**f**) Immunoblot with anti-GFP antibody validates the presence of YFP-HAM2 (YPET-HAM2) in both nuclear lysate and nuclear proteins

immunoprecipitated with GFP-Trap from *ham1,2,4* [*pHAM2::YFP-HAM2*] line used in ChIP experiment (Fig. 2, n and o).

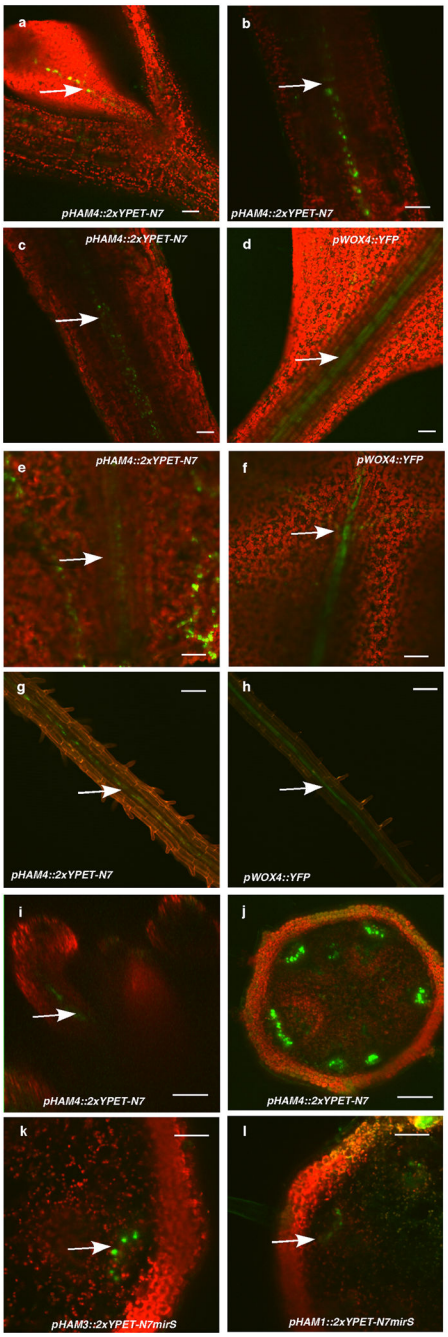

Extended Data Figure 7.

Expression patterns of *HAM*genesin comparison to *WOX4.* (**a**) *pHAM4::2xYPET-N7* (green, arrow indicated) is expressed in procambium cells of the first leaf. (**b**) *pHAM4::2xYPET-N7* (green, arrow indicated) is expressed in vasculature in the 7-day-old hypocotyl. (**c**–**h**) Comparison of *pHAM4::2xYPET-N7* (green, arrow indicated) and *pWOX4::YFP* (green,

arrow indicated) expression patterns in vasculature cells in the 7-d-old leaf petiole (**c–d**),20-d-old leaf petiole (**e–f**) and 7-d-old root (**g–h**). (**i**) Orthogonal view of *pHAM4::2xYPET-N7* (green, arrow indicated) expression in flower vasculature. (**j**) Procambium-specific expression of p*HAM4::2xYPET-N7* in stems from 1cm bolting plants. (**k–l**) Procambium-specific expression of *pHAM3::2xYPET-N7mirS* (**k**) and *pHAM1::2xYPET-N7mirS* (**l**) in transverse sections of stems from 1 cm bolting plants. Red in (**a–f**, **i–l**) represents chlorophyll autofluorescence, and represents PI staining in (**g–h**). Bars = 50μm in (**a, h–i, k–l**); 100μm in (**b–g, j**).

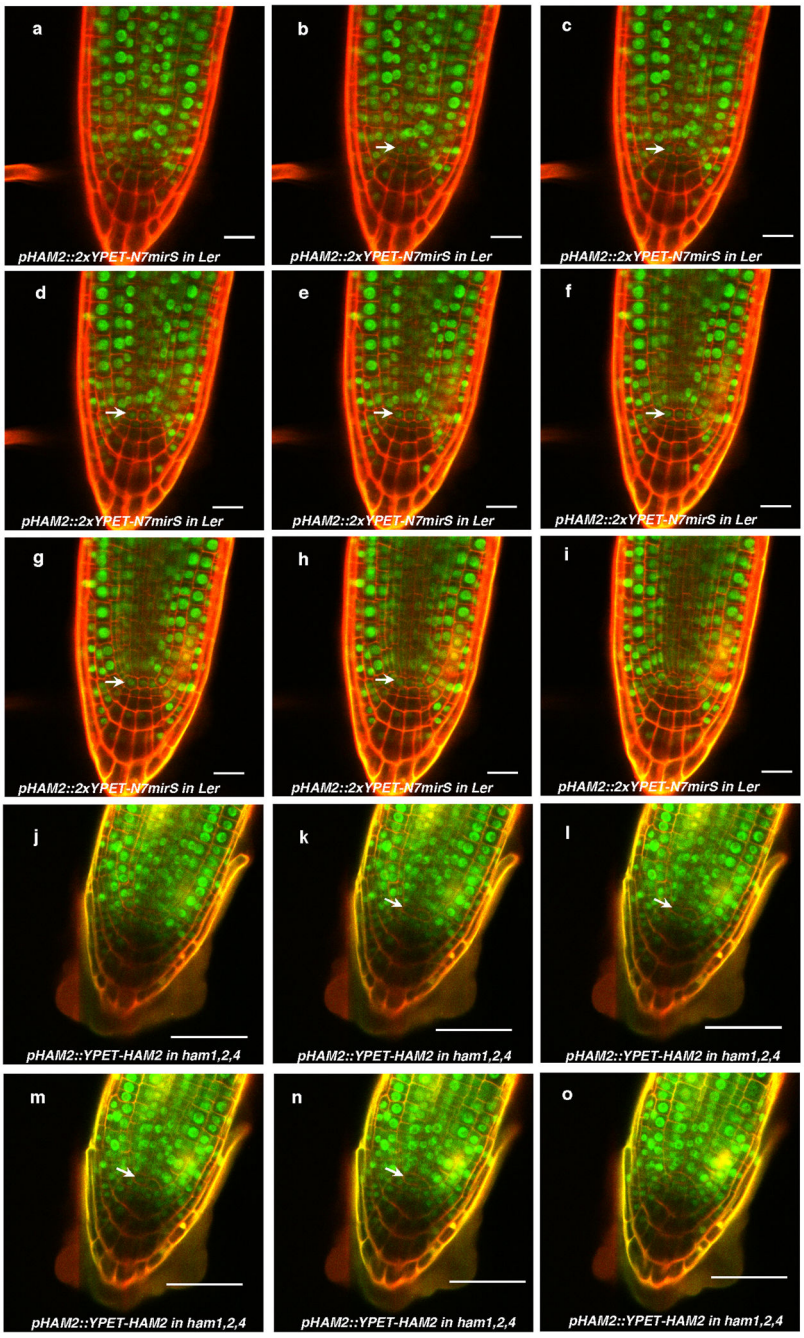

Extended Data Figure 8.

Expression patterns of *HAM2* transcriptional and translational reporters in root meristems. (**a–i**) Complete stacks of confocal sections through the root tip demonstrate that *pHAM2::2xYPET-N7mirS* (green) is expressed in the QC cells (arrow indicated) and cells above the QC within the root meristem. (**j–o**) Expression patterns of HAM2 translational reporters in *ham1,2,4* root meristems. Complete stacks of confocal sections through the root tip demonstrate that *pHAM2:YPET-HAM2* (green) is present in the QC cells (arrow

indicated) and the cells above the QC within the root meristem in the *ham1,2,4* mutant. In all figures cellular outlines were stained with PI (red). Bars = 20μm (**a–i**), 50μm (**j–o**).

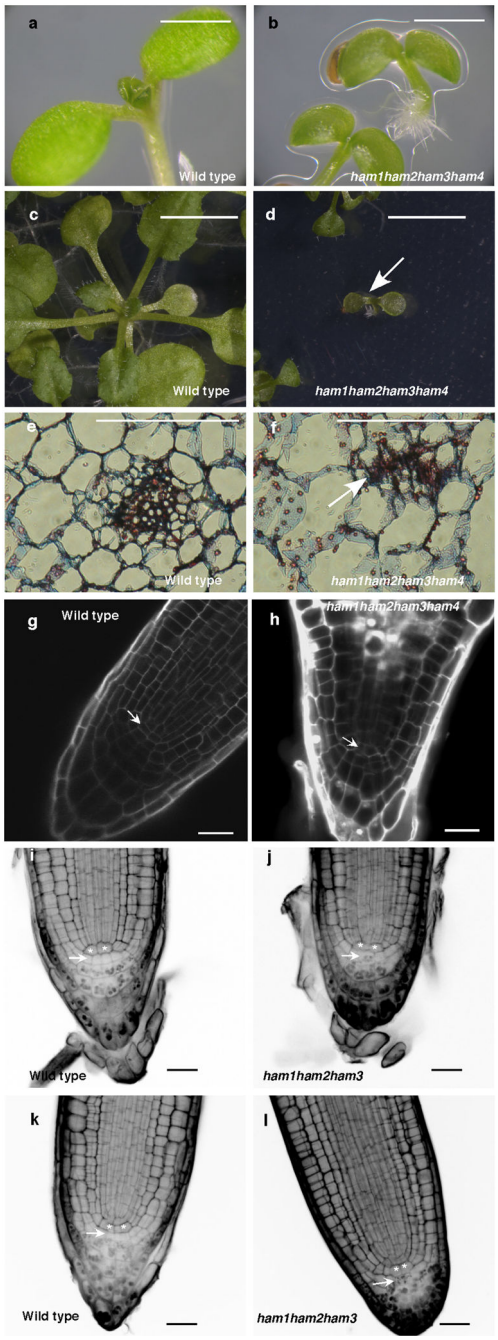

Extended Data Figure 9.

HAM family regulates various stem cell niches. (**a–d**) Growth arrest of *ham1;2;3;4* at the seedling stage. Imaging of L*er* wild type (WT) (**a**) and homozygous *ham1;2;3;4* (**b**) seedlings at 7 days after germination (DAG). Imaging of WT (**c**) and homozygous *ham1;2;3;4* (**d**) (arrow indicated) seedlings at 26 DAG. (**e–f**) Transverse section of leaves

from WT (**e**) and *ham1;2;3;4* (**f**) at 7 DAG. Arrow in (**f**) indicates undifferentiated/ undetermined cell mass. (**g–h**) Confocal imaging of root meristem from WT (**g**) and *ham1;2;3;4* (**h**) seedlings at 7 DAG. *ham1;2;3;4* displayed enlarged cells with abnormal shapes at the QC (arrow indicated) and columella stem cell (CSC) positions. Cellular outlines (**g–h**) were visualized with PI staining (white). (**i–l**) mPS-PI[41] stains indicate that HAM genes regulate root cell differentiation. Some CSCs (arrow indicated) undergo differentiation with starch accumulated and stained in homozygous *ham1;2;3* (**j, l**), but none of them can be stained in L-er wild type (**i, k**). Asterisks mark the QC cells. Bars= 5mm (**c–d**), 1 mm in (**a–b**, **e–f),** 20 μm in (**g–l**).

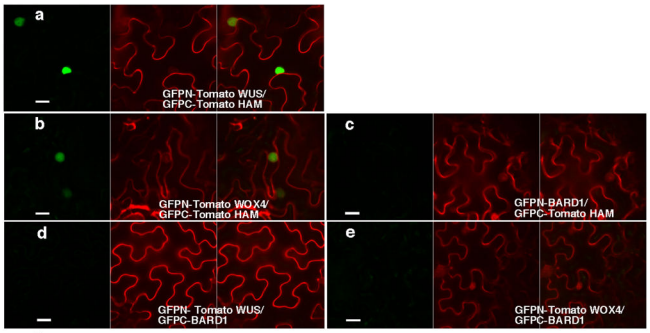

f

```
AtHAM1          ---MPLSFERFQGEGVFGLSSSSFYS---------------DSQKIWSNQDKTEAKQEDL    42
PetuniaHAM      MIAIPQ-----GAKGVLGVSSFMPSISSEEQICKKDANFARNDPQICKKDGNFARNEPQI    55
TomatoHAM       MIVIPQ-SNNLPAKGVLGVSGFVPSISSSS-----------------------SPEASI    35
                   :*       .:**:*:*.                                  : .:

AtHAM1          GYVVGGFL-PEPTSVLDALRSPSPLASYSSTTTTLSSSHGGGGTTVTNTTVT--AGD---    96
PetuniaHAM      CKKEGNFTRNEPVSVLD-TRSPSPSS--SS--CSYA---------------GKVEGQKEE    95
TomatoHAM       CKKDANFTRNEPVSVLD-TRSPSPSASSSS--CSYGAQHGGN-TAVPGVGSGKTDGRKEE    91
                    . *   **.****  ***** :  **   : .                  *

AtHAM1          ----------DNNNNKCSQMGLDDLDGVLSASSPGQEQSILRLIMDP----GSAF-----   137
PetuniaHAM      LVKELQPFPLVGLEPEKCSLGFGDLDNLLPEL-CGADQTLLRWISGDMEDPSVSLKQLLL   154
TomatoHAM       LVTELEPFT-VGLEPEKSVLGFGDLDNLLPEF-AGSDQSFLRWISGDVEDPSVSLKQLLN   149
                          : : . :*: *** :*     * :*::** *       . ::

AtHAM1          GVFDPGFGFGSGSGPVSAP----VSDN-----SNLLCNFPFQEITNPAEALINPSN----   184
PetuniaHAM      GGNANGF-HGSSGFEASAAGSLVHTDNVSFSGSDVSLNANIEKIGSVIDSNGRPSNGFDY   213
TomatoHAM       GDLGCGVSLQSSGFEVSATGSLAHSDNVSFSGSNICLNANIEKLSSVIDSINSRNNNFEN   209
                *    *.   *..  .**      :**     *::  *  :::: .  ::    .*

AtHAM1          ----------------------------------------HCLFY---------------NPP   192
PetuniaHAM      LNANLYAKSLPLPPASSFQEQKLGQKPQSFS----PNQALFQNASYGNMFDSSSYDDTNQ   269
TomatoHAM       PNVNP----------------SLEQKPQPFGPQVMANQTQFQNAACVNIFGSSSYD-INQ   252
                                                :  *

AtHAM1          LSPPAKRFNSGSLHQPVFPLSDPDPGHDP-----VRRQH----QFQFPFYHNNQQQQFPS   243
PetuniaHAM      EQPPSKRHNSGTLGSSVGGLLPKVPFFDPSGDLSMRRQLLGEMQQHFNLLPPQQFQPKPL   329
TomatoHAM       EQPPPKRHNSGTLG---GALLPKVPFFDANCDFMLRKQPLGQMQPQVNLLPPHQFQPKPL   309
                 .** **.***:*       *    * .*      :*:*     * :. :   .* *  *

AtHAM1          ----SSSSTAVAMVPVPSPGMAGDDQSVIIEQLFNAAELIGTTGNNNGDHTVLAQGILAR   299
PetuniaHAM      IVPKLEAACGGGNGSLMVPRHQQQEQQFIYDQIFQASELLLAG------HFSNAQMILAR   383
TomatoHAM       IVPKLEAAGGGGNGNLMVPRHQLQEQQFIYDQIFQASELLLAG------QFSNAQMILAR   363
                     .:: . .   :  *    ::*..* :*:*:*:**: :       :   ** ****

AtHAM1          LNHHLNTSSNHKSPFQRAASHIAEALLS-----LIHNESSPPLITPENLILRIAAYRSFS   354
PetuniaHAM      LNQQLSP---IGKPFKRAAFYFKEALQLPFLLPCTSTFLPPRSPTPFDCVLKMDAYKSFS   440
TomatoHAM       LNQQLSP---IGKPSRRAAFYIKEALQLPFLLPCTSTFLPPRSPTPFDCVLKMDAYKAFS   420
                **::*.      .* :*** :: ***          .   *   ** : :*:: **::**

AtHAM1          ETSPFLQFVNFTANQSILESCNESGFDRIHIIDFDVGYGGQWSSLMQELASGVGGRRRNR   414
PetuniaHAM      EVSPLIQFMNFTSNQAILEALG--DVERIHIIDFDIGFGAQWSSFMQELPSSN-----RK   493
TomatoHAM       EISPLIQFMNFTSNQAILEALG--DAEQIHIIDFDIGFGAQWSSFMQELPSSN-----RK   473
                * **::**:***:**:***:       ::*******:*:*.****:**** *.      .:

AtHAM1          ASSLKLTVFAPPPSTVSDEFELRFTEENLKTFAGEVKIPFEIELLSVELLLNPAYWPLSL   474
PetuniaHAM      ATSLKITAFASPSTHH--SVEIAIMHESLTQFANDAGIRFELEVINLDTFDPKSYPLSSL   551
TomatoHAM       ATSLKITAFASPSTHH--SIEIGIMHESLTQFANDAGIRFELEVINLDSFDPKSYPLSTL   531
                *:***:*.** * :    ..*: : .*.*. ** :. * **:*::.:: :   :*   :*

AtHAM1          RSSEKEAIAVNLPVNSVASGY--LPLILRFLKQLSPNIVVCSDRGCDRNDAPFPNAVIHS   532
PetuniaHAM      RSSDCEAIAINFPIWSISSCLFAFPSLLHYMKQLSPKIIVSLERGCERTELPLKHHLLHA   611
TomatoHAM       RSSECEAIAINFPIWSISSCPFAFPSLLHCMKQLSPKVVVSLERGCERTELPLKHHLIHA   591
                ***: ****:*:*: *::*    :* :*: :*****:::*. :***:*.: *: . ::*:

AtHAM1          LQYHTSLLESLDANQNQD--DSSIERFWVQPSIEKLLMKRHRWIERSPPWRILFTQCGFS   590
PetuniaHAM      LQYYEILLASIDAANVTPEIGKKIEKSLLLPSIENMVLGRLRSPDRMPQWRNLFASAGFS   671
TomatoHAM       LQYYETLLASIDAANITPDIGKKIERSLFQPSIENMILGRLRSSDRMPPWRNLFASAGFS   651
                ***:  ** *:** :       ..**:  . ****:::: * *  :* * ** **:..***

AtHAM1          PASLSQMAEAQAECLLQRNPVRGFHVEKRQSSLVMCWQRKELVTVSAWKC----------   640
PetuniaHAM      PVAFSNLTEIQAECVVKRTQVGGFHVEKRQSSLVLCWKQQELLSALTWRC----------   721
TomatoHAM       PVAFSNMTEIQAECVVKRTQVGGFHVQKRQTSLVLCWKQQELLSAVTWRCRGAFLLKPEE   711
                *.::*:::* ****:::*. * ****:***:***:**:::**::. :*:*
```

Extended Data Figure 10.

Interaction between WOX and HAM homologs from tomato (Solanum lycopersicum). Bimolecular fluorescence complementation (BiFC) analyses in tobacco transient assays demonstrated that tomato WUS (Gene ID: 543793) physically interacted with a putative tomato HAM homolog (LEFL2052P11) (**a**) identified based on its sequence homology to HAM from *Arabidopsis* and Petunia (**f**), and tomato WOX4[10] (Gene ID: 100301933) physically interacted with the putative tomato HAM homolog (**b**). BARD1 protein is included as a negative control (**c–e**). Left panel: GFP channel; middle panel: PI staining channel; right panel: merged channels. Scale bar = 20 μm.(**f**) Amino acid sequence alignment of a putative tomato HAM, *Arabidopsis* HAM1 and petunia HAM using Clustal Omega. Asterisks: same amino acids; dots: similar amino acids.

Supplementary Material

Refer to Web version on PubMed Central for supplementary material.

Acknowledgments

The authors are grateful to Dr. R. Deshaies for his generous support with the protein purification and pull-down experiments, to Dr. D. Rees for sharing the 96-well format luminometer, to Drs. T. Laux, T. Greb, and X. Deng for sharing published reagents, to Drs. K. Sugimoto and A. Roeder for the help with the histology experiments and critical reading of the manuscript, to Dr. A. Sampathkumar for the suggestion on confocal imaging, and to A. Garda and L. Wang for technical support. Scanning electron microscopy was performed at the Applied Research Center of the College of William and Mary with technical assistance from B. Robertson. This work was funded by NIH grant R01 GM104244and by the Howard Hughes Medical Institute and the Gordon and Betty Moore Foundation (through Grant GBMF3406) to Elliot M. Meyerowitz, by a Caltech Gosney Postdoctoral Fellowship to Yun Zhou, by National Institutes of Health Grants GM094212, GM056006, and GM067837 to Steve A. Kay, and was aided by a grant from The Jane Coffin Childs (JCC) Memorial Fund for Medical Research to Xing Liu, a JCC fellow.

References

1. Meyerowitz EM. Genetic control of cell division patterns in developing plants. Cell. 1997; 88:299–308. [PubMed: 9039256]
2. Sablowski R. The dynamic plant stem cell niches. Current opinion in plant biology. 2007; 10:639–644. [PubMed: 17692560]
3. Miyashima S, Sebastian J, Lee JY, Helariutta Y. Stem cell function during plant vascular development. The EMBO journal. 2013; 32:178–193. [PubMed: 23169537]
4. Dinneny JR, Benfey PN. Plant stem cell niches: standing the test of time. Cell. 2008; 132:553–557. [PubMed: 18295573]
5. Laux T, Mayer KF, Berger J, Jurgens G. The WUSCHEL gene is required for shoot and floral meristem integrity in Arabidopsis. Development. 1996; 122:87–96. [PubMed: 8565856]
6. Mayer KF, et al. Role of WUSCHEL in regulating stem cell fate in the Arabidopsis shoot meristem. Cell. 1998; 95:805–815. [PubMed: 9865698]
7. Schoof H, et al. The stem cell population of Arabidopsis shoot meristems in maintained by a regulatory loop between the CLAVATA and WUSCHEL genes. Cell. 2000; 100:635–644. [PubMed: 10761929]
8. Sarkar AK, et al. Conserved factors regulate signalling in Arabidopsis thaliana shoot and root stem cell organizers. Nature. 2007; 446:811–814. [PubMed: 17429400]
9. Hirakawa Y, Kondo Y, Fukuda H. TDIF peptide signaling regulates vascular stem cell proliferation via the WOX4 homeobox gene in Arabidopsis. The Plant cell. 2010; 22:2618–2629. [PubMed: 20729381]
10. Ji J, et al. WOX4 promotes procambial development. Plant physiology. 2010; 152:1346–1356. [PubMed: 20044450]

11. Suer S, Agusti J, Sanchez P, Schwarz M, Greb T. WOX4 imparts auxin responsiveness to cambium cells in Arabidopsis. The Plant cell. 2011; 23:3247–3259. [PubMed: 21926336]
12. Nardmann J, Reisewitz P, Werr W. Discrete shoot and root stem cell-promoting WUS/WOX5 functions are an evolutionary innovation of angiosperms. Molecular biology and evolution. 2009; 26:1745–1755. [PubMed: 19387013]
13. van der Graaff E, Laux T, Rensing SA. The WUS homeobox-containing (WOX) protein family. Genome Biol. 2009; 10:248. [PubMed: 20067590]
14. Pruneda-Paz JL, et al. A genome-scale resource for the functional characterization of Arabidopsis transcription factors. Cell reports. 2014; 8:622–632. [PubMed: 25043187]
15. Stuurman J, Jaggi F, Kuhlemeier C. Shoot meristem maintenance is controlled by a GRAS-gene mediated signal from differentiating cells. Genes Dev. 2002; 16:2213–2218. [PubMed: 12208843]
16. Engstrom EM, et al. Arabidopsis homologs of the petunia hairy meristem gene are required for maintenance of shoot and root indeterminacy. Plant physiology. 2011; 155:735–750. [PubMed: 21173022]
17. Schulze S, Schafer BN, Parizotto EA, Voinnet O, Theres K. LOST MERISTEMS genes regulate cell differentiation of central zone descendants in Arabidopsis shoot meristems. The Plant journal. 2010; 64:668–678. [PubMed: 21070418]
18. Graf P, et al. MGOUN1 encodes an Arabidopsis type IB DNA topoisomerase required in stem cell regulation and to maintain developmentally regulated gene silencing. The Plant cell. 2010; 22:716–728. [PubMed: 20228247]
19. Llave C, Xie Z, Kasschau KD, Carrington JC. Cleavage of Scarecrow-like mRNA targets directed by a class of Arabidopsis miRNA. Science. 2002; 297:2053–2056. [PubMed: 12242443]
20. Busch W, et al. Transcriptional control of a plant stem cell niche. Developmental cell. 2010; 18:849–861. [PubMed: 20493817]
21. Yadav RK, et al. WUSCHEL protein movement mediates stem cell homeostasis in the Arabidopsis shoot apex. Genes & development. 2011; 25:2025–2030. [PubMed: 21979915]
22. Nawy T, et al. Transcriptional profile of the Arabidopsis root quiescent center. The Plant cell. 2005; 17:1908–1925. [PubMed: 15937229]
23. Brady SM, et al. A high-resolution root spatiotemporal map reveals dominant expression patterns. Science. 2007; 318:801–806. [PubMed: 17975066]
24. Fletcher JC, Brand U, Running MP, Simon R, Meyerowitz EM. Signaling of cell fate decisions by CLAVATA3 in Arabidopsis shoot meristems. Science. 1999; 283:1911–1914. [PubMed: 10082464]
25. Gordon SP, Chickarmane VS, Ohno C, Meyerowitz EM. Multiple feedback loops through cytokinin signaling control stem cell number within the Arabidopsis shoot meristem. Proceedings of the National Academy of Sciences of the United States of America. 2009; 106:16529–16534. [PubMed: 19717465]
26. Walter M, et al. Visualization of protein interactions in living plant cells using bimolecular fluorescence complementation. The Plant journal. 2004:428–438. [PubMed: 15469500]
27. Voinnet O, Rivas S, Mestre P, Baulcombe D. An enhanced transient expression system in plants based on suppression of gene silencing by the p19 protein of tomato bushy stunt virus. The Plant journal. 2003; 33:949–956. [PubMed: 12609035]
28. Ohashi-Ito K, Bergmann DC. Arabidopsis FAMA controls the final proliferation/differentiation switch during stomatal development. The Plant cell. 2006; 18:2493–2505. [PubMed: 17088607]
29. Curtis MD, Grossniklaus U. A gateway cloning vector set for high-throughput functional analysis of genes in planta. Plant physiology. 2003; 133:462–469. [PubMed: 14555774]
30. Pierce NW, et al. Cand1 promotes assembly of new SCF complexes through dynamic exchange of F box proteins. Cell. 2013; 153:206–215. [PubMed: 23453757]
31. Harper S, Speicher DW. Current protocols in protein science. 2008; Chapter 6(Unit 6.6)
32. Huang X, et al. Arabidopsis FHY3 and HY5 positively mediate induction of COP1 transcription in response to photomorphogenic UV-B light. The Plant cell. 2012; 24:4590–4606. [PubMed: 23150635]

33. Carlsbecker A, et al. Cell signalling by microRNA165/6 directs gene dose-dependent root cell fate. Nature. 2010; 465:316–321. [PubMed: 20410882]
34. Wang L, Mai YX, Zhang YC, Luo Q, Yang HQ. MicroRNA171c-targeted SCL6-II, SCL6-III, and SCL6-IV genes regulate shoot branching in Arabidopsis. Molecular plant. 2010; 3:794–806. [PubMed: 20720155]
35. Barrell PJ, Conner AJ. Minimal T-DNA vectors suitable for agricultural deployment of transgenic plants. BioTechniques. 2006; 41:708–710. [PubMed: 17191614]
36. Heisler MG, et al. Patterns of auxin transport and gene expression during primordium development revealed by live imaging of the Arabidopsis inflorescence meristem. Current biology. 2005; 15:1899–1911. [PubMed: 16271866]
37. Reddy GV, Meyerowitz EM. Stem-cell homeostasis and growth dynamics can be uncoupled in the Arabidopsis shoot apex. Science. 2005; 310:663–667. [PubMed: 16210497]
38. Sugimoto K, Jiao Y, Meyerowitz EM. Arabidopsis regeneration from multiple tissues occurs via a root development pathway. Developmental cell. 2010; 18:463–471. [PubMed: 20230752]
39. Roeder AH, Ferrandiz C, Yanofsky MF. The role of the REPLUMLESS homeodomain protein in patterning the Arabidopsis fruit. Current biology. 2003; 13:1630–1635. [PubMed: 13678595]
40. Bowler C, et al. Chromatin techniques for plant cells. The Plant journal. 2004; 39:776–789. [PubMed: 15315638]
41. Truernit E, et al. High-resolution whole-mount imaging of three-dimensional tissue organization and gene expression enables the study of Phloem development and structure in Arabidopsis. The Plant cell. 2008; 20:1494–1503. [PubMed: 18523061]

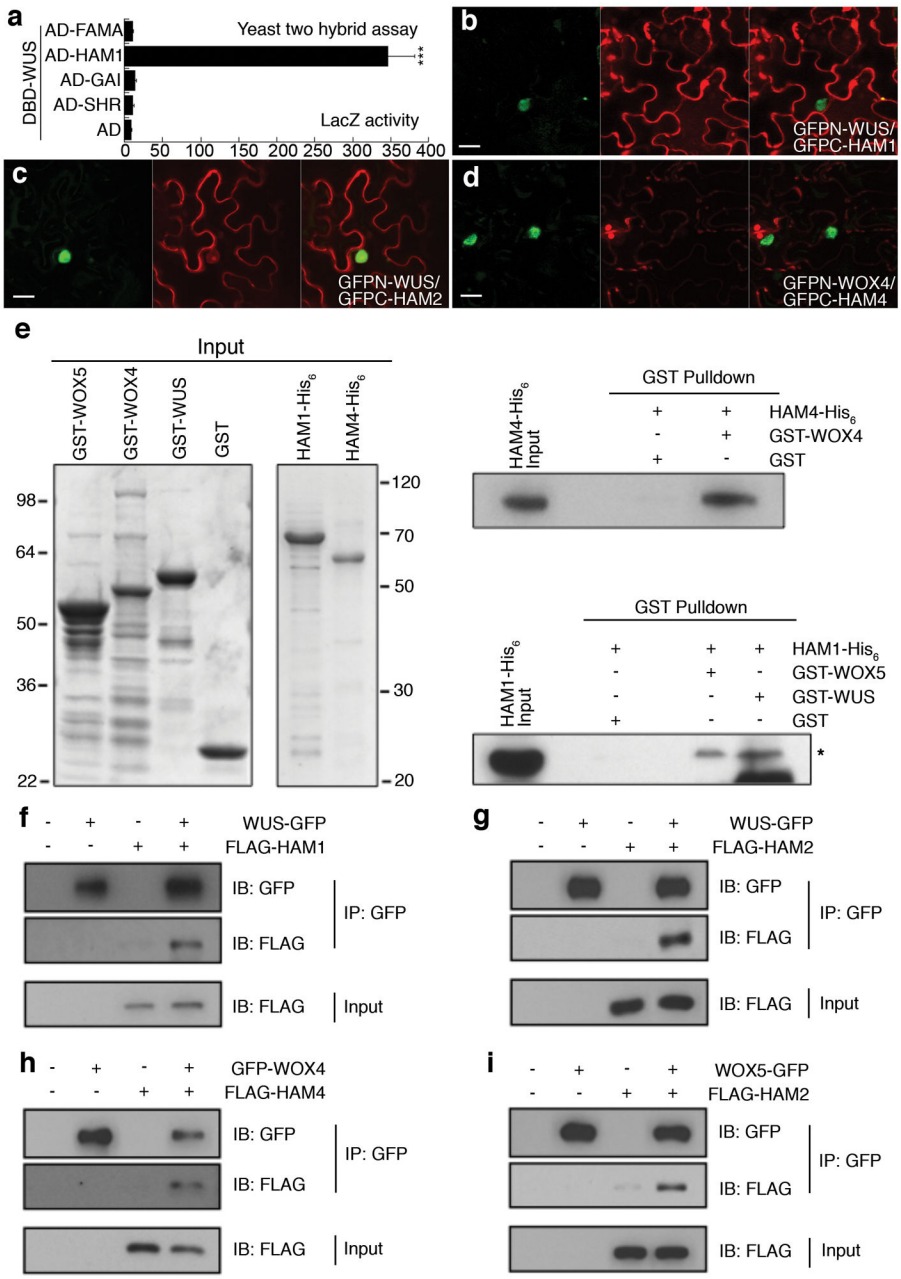

Figure 1. WUS/WOX and HAM family proteins physically interact

(**a**) LacZ activity of yeast-two-hybrid assays. Error bar = mean ± sem (n=3biological replicates). ***, P<0.001(two-tailed t-test). (**b**–**d**) Bimolecular fluorescence complementation in tobacco. Panels (left to right): GFP; propidium iodide (PI) staining; merged channels. Scale bar = 20μm.(**e**) SDS-PAGE of input recombinant proteins stained by Coomassie Blue (left), and pull down of His_6-tagged HAM proteins through GST-tagged WUS/WOX proteins detected by immunoblotting with anti-His antibody (right). Asterisk: HAM1-His_6band. (**f**–**j**) Co-immunoprecipitation of WUS-GFP and FLAG-HAM1 (**f**), WUS-GFP and FLAG-HAM2 (**g**), GFP-WOX4 and FLAG-HAM4(**h**), WOX5-GFP and FLAG-HAM2(**i**) (see Methods).

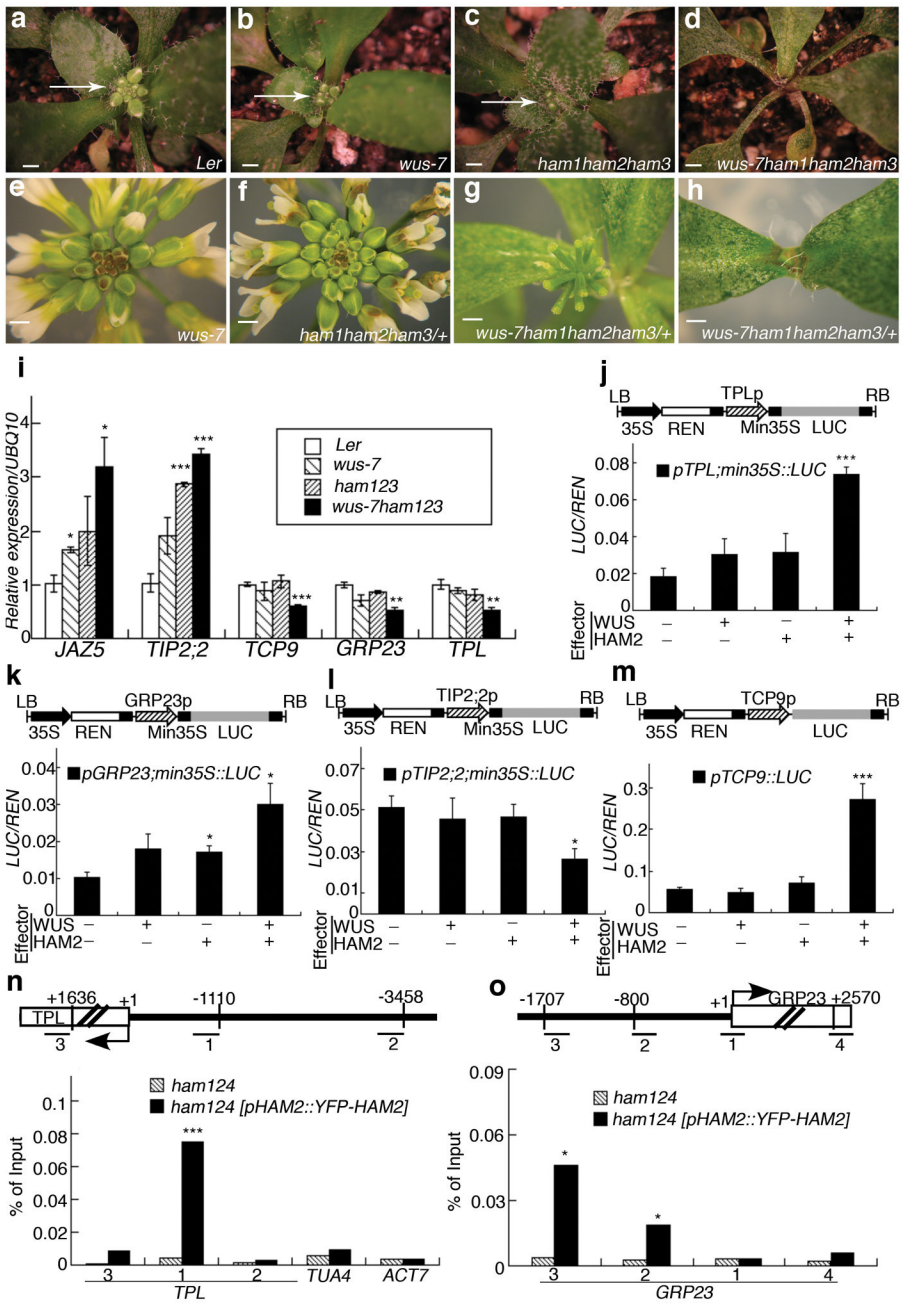

Figure 2. *WUS* and *HAM* family genes cooperatively control the shoot stem cell niche and co-regulate a common gene set

Shoot apices (**a–d**) (arrows) and inflorescence structures(**e–h**)of plants in indicated genotypes. Bars = 2 mm in (**a–h**).(**i**) RT-PCR quantification of WUS and HAM target gene expression in indicated genotypes. Error bar = mean ± sem(n=3 biological replicates). (**j–m**) LUC/REN activity in tobacco cells co-transformed with different reporter constructs (structured above each graph) and indicated effectors(see Methods). Min35S: 60 base pair 35S minimum element, REN: Renilla luciferase, LUC: firefly luciferase, LB/RB: T-DNA left or right border. Error bar = mean ± sem(n=3biological replicates). (**n–o**) Chromatin

Immunoprecipitation of HAM2 protein with *TPL* or *GRP23* chromatin regions, with ampliconlocations (Bars with numbers) diagrammed above each graph. The ChIP experiments were repeated three times using independent biological replicates with similar results, and one representative data set is shown.*, P<0.05; **, P<0.01; ***, P<0.001(two-tailed t-test) in (**i–o**).

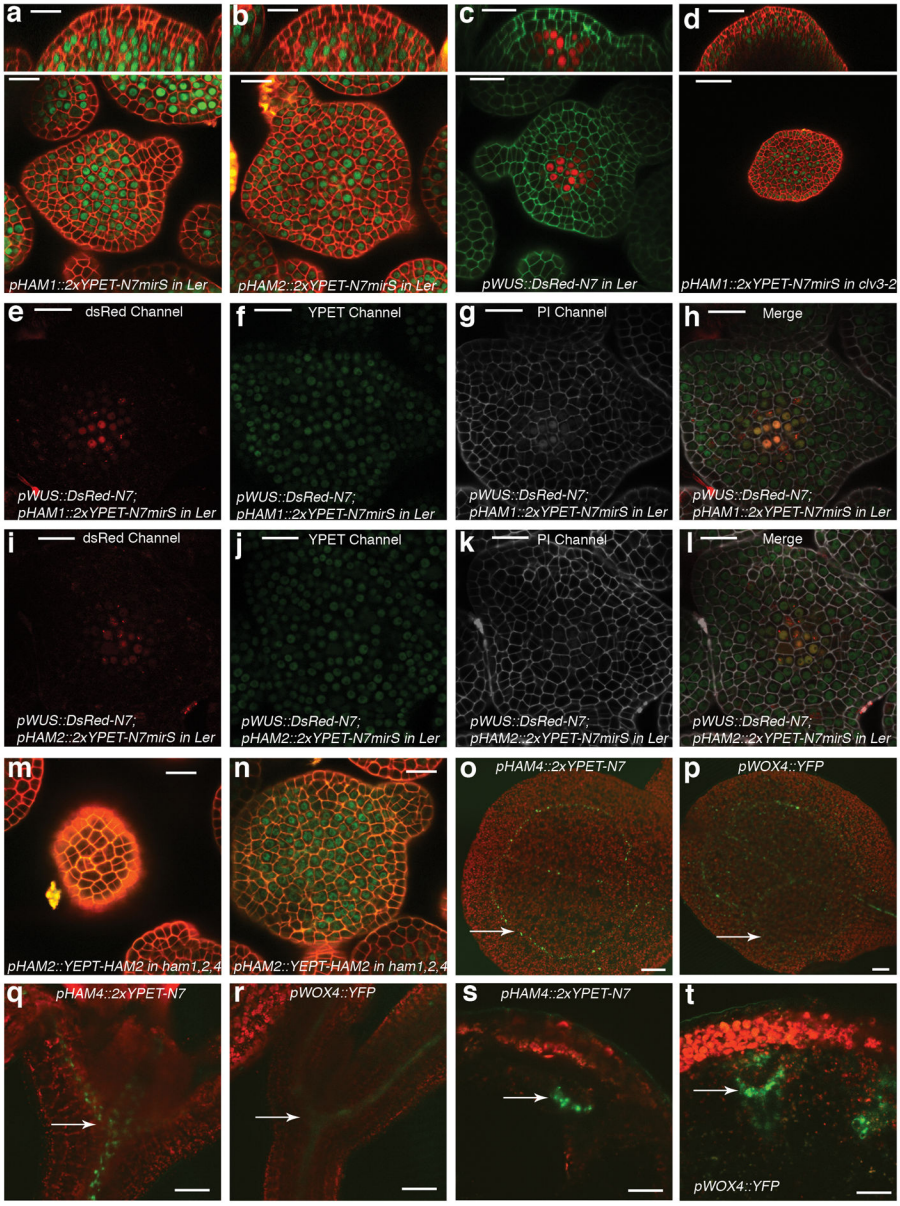

Figure 3. *HAM* and *WUS*/*WOX* expression domains overlap

Expression of (**a**) *pHAM1::2xYPET-N7microRNAsensitive* marker (*pHAM1::2xYPET-N7mirS*) (green), (**b**) *pHAM2::2xYPET-N7mirS* (green), (**c**) *pWUS::DsRed-N7* (red) in L-*er* inflorescence meristem (IM), and (**d**) *pHAM1::2xYPET-N7mirS* (green) marker in a *clv3-2* IM. Orthogonal (upper panels) and transverse section (lower panels) views of the same plant are shown. (**e**–**l**) Overlapping expression patterns of *pWUS::DsRed-N7* with *pHAM1::2xYPET-N7mirS* or *pHAM2::2xYPET-N7mirS* in the same shoot meristems (see Methods). Panels (from left to right): dsRed (red); YPET (green); PI (gray); merged channels. (**m**–**n**) Expression of *pHAM2::YPET-HAM2* translation almarker (green) in L1 (**m**) and L3 (**n**) of the same *ham1,2,4* SAM.(**o**–**t**) Overlapping expression patterns of *pHAM4::2xYPET-N7*and *pWOX4::YFP* (green, arrows) in the provascular and procambium

cells in cotyledons (**o**–**p**), seedlings (**q**–**r**), and stem transverse sections (**s**–**t**). PIcounter stain: red (**a**–**b, d, m**–**n**), green (**c**), gray (**g**–**h, k**–**l**). Chlorophyll autofluorescence: red (**o**–**t**). Bars = 50 μm in (**d, s**–**t**); 200 μm in (**o**); 100 μm in (**p**–**r**); 20 μm in (**a**–**c, e**–**n**).

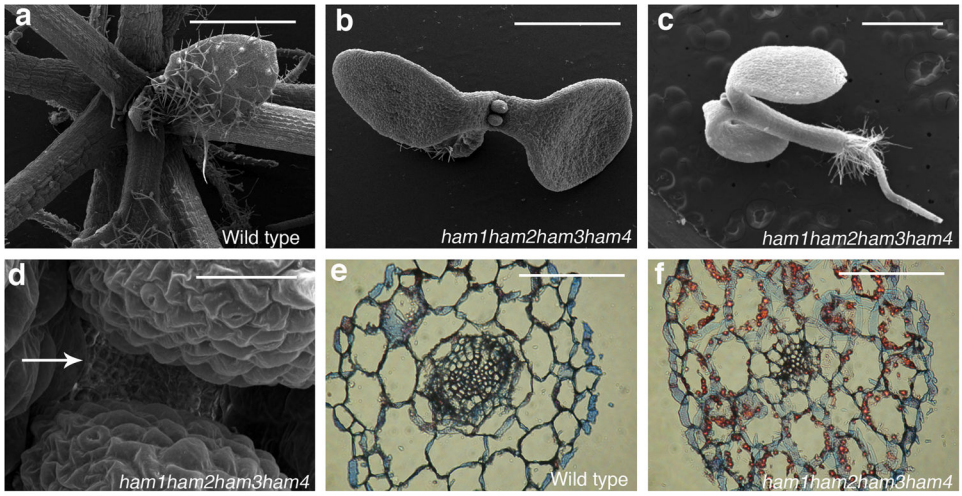

Figure 4. HAM family members are essential for various plant stem cell activities

Scanning electron microscopic imaging of WT (**a**) and *ham1*, *ham2*, *ham3*, *ham4* (**b**–**d**) seedlings (26 DAG). Arrow: *ham1;2;3;4*lacking a functional SAM.(**e**–**f**) Transverse sections of WT and *ham1;2;3;4*hypocotyls (7 DAG). Bars = 1 mm in (**a**–**c, e**–**f**), 50 μm in (**d**).